

# Thou shalt not tunnel

## Complex instantons and tunneling suppression in deformed quantum mechanics

---

Jie Gu<sup>a</sup> and Marcos Mariño<sup>b</sup>

<sup>a</sup>*School of physics & Shing-Tung Yau Center  
Southeast University, Nanjing 211189, P. R. China*

<sup>b</sup>*Département de Physique Théorique et Section de Mathématiques  
Université de Genève, Genève, CH-1211 Switzerland*

ABSTRACT: The quantization of the Seiberg–Witten curve of  $\mathcal{N} = 2$  super Yang–Mills theory leads to a deformation of one-dimensional quantum mechanics with unconventional behavior. Most notably, quantum tunneling is suppressed at special points in parameter space. In this paper we examine these deformed models in the case of double-well and cubic potentials, and we find that they have a rich phase structure. In what we call the strong coupling phase, the theory behaves like conventional quantum mechanics, instantons are real, and tunneling is not suppressed. In the weak coupling phase, the instantons responsible for tunneling become complex, and tunneling suppression takes place at the so-called Toda lattice points. At the critical point between the two phases, which corresponds to a monopole point in super Yang–Mills theory, the non-perturbative amplitudes display an anomalous scaling as a function of  $\hbar$ . This phase structure reflects the physics of the underlying super Yang–Mills theory and can be regarded as a physical manifestation of wall-crossing behavior of the BPS spectrum, which we determine in our problem by using resurgent techniques.

---

## Contents

<b>1</b>	<b>Introduction</b>	<b>1</b>
<b>2</b>	<b>Deformed quantum mechanics</b>	<b>3</b>
<b>3</b>	<b>Strong coupling phase</b>	<b>5</b>
3.1	Nonperturbative effects from instantons	5
3.2	Instanton contribution in deformed quantum mechanics	7
3.3	From instantons to WKB	17
<b>4</b>	<b>Weak coupling phase and tunneling suppression</b>	<b>19</b>
4.1	Complexifying the instantons	19
4.2	Resurgent analysis and Stokes constants	23
4.3	Comparison to the exact quantization conditions	30
<b>5</b>	<b>The critical theories</b>	<b>34</b>
<b>6</b>	<b>Conclusions</b>	<b>37</b>

---

## 1 Introduction

Tunneling through a potential barrier is a quintessential quantum phenomenon with no counterpart in classical physics, and its importance was recognized from the very beginning of quantum theory [1]. In addition, tunneling leads to some of the most famous non-perturbative effects in physics, i.e. effects that are exponentially small in  $\hbar$  (or the coupling constant). The best known examples are tunneling between two degenerate minima in a double-well potential, which leads to a non-perturbative energy gap, and tunneling in a metastable state, which leads to a non-perturbative imaginary part in the energy of the states (see e.g. [2, 3] for textbook presentations of these phenomena in one-dimensional quantum mechanics, and [4, 5] for a recent clarifying discussion.)

Physicists have been also intrigued by the possibility that quantum tunneling be suppressed in certain circumstances, and various scenarios where this happens have been proposed. One possibility is to add an external periodic field to a situation where tunneling occurs (for example, a double-well potential) [6]. The Hamiltonian becomes time-dependent and tunneling gets suppressed in what has been dubbed coherent destruction of tunneling (CDT). A different mechanism occurs in spin systems, where tunneling is suppressed due to the destructive interference between tunneling paths [7, 8]. In particular, in [8] tunneling is suppressed for a discrete set of values of a control parameter, involving an external magnetic field. More recently, it has been shown that tunneling is suppressed in conventional double-well potentials in two dimensions, for certain values of an external magnetic field [9]. In the examples involving spin systems, the suppression of tunneling can be understood in terms of complex instantons in the coherent path integral for spins, where the complexification is due to a Berry phase. Presumably, the suppression observed in [9] can be also understood in terms of complex instantons, since the external magnetic field

introduces a phase in the instanton paths (akin to the Aharonov–Bohm effect). Both examples involve tunneling paths in two dimensions, either in the two-dimensional sphere describing spin coherent states, or in real space. CDT can occur in one dimension, but the instanton picture is less clear due to the presence of a time-dependent Hamiltonian.

A different and potentially simpler scenario where quantum tunneling is suppressed was discovered in [10]. This scenario involves a one-dimensional Hamiltonian with an arbitrary polynomial potential of degree  $N$ , but instead of the conventional non-relativistic kinetic term  $\mathbf{p}^2/2$  one has a deformation to  $\cosh(\mathbf{p}) - 1$ . With such a modified kinetic term, the conventional Schrödinger differential equation for the wavefunction becomes a finite difference equation. In [10] it was shown that, when the polynomial potential in the deformed model is the familiar double-well potential, tunneling between the two wells is completely suppressed for special values of the parameters in the potential, and one finds doubly-degenerate energy states. Tunneling is also suppressed in the related example of resonances in an unbounded potential, like e.g. a cubic potential. This is manifested in the vanishing of the imaginary part of the energy for certain values of the parameters.

Why are such deformed quantum-mechanical models interesting? One motivation for their study in [10] is that they can be regarded as a quantization of the spectral curve of the periodic Toda lattice with  $N$  particles, or equivalently [11], of the Seiberg–Witten (SW) curve of  $\mathcal{N} = 2$  Yang–Mills theory with gauge group  $SU(N)$  [12]. It is then expected that the properties of the deformed quantum mechanics are manifestations of the rich properties of these underlying systems. Importantly for us, [10] conjectured that the suppression of tunneling occurs precisely when the parameters of the polynomial potential correspond to the eigenvalues of the quantum periodic Toda lattice. Another motivation for [10] comes from the TS/ST (topological string/spectral theory) correspondence [13–15], which provides conjectural exact quantization conditions (EQCs) for many spectral problems based on a quantum spectral curve. The quantization of the SW curve turns out to be a relatively simpler case of the correspondence, and [10] proposed EQCs in closed form for any polynomial potential. These conditions imply in turn the suppression of quantum tunneling at the Toda lattice points, and were tested numerically in [10].

In this paper we would like to provide a better understanding of the suppression of quantum tunneling in these deformed quantum-mechanical models by using an instanton approach. We will focus on the double-well and cubic potentials, depending on a control parameter, and we will show that they have two different phases as this parameter is changed. The phase structure concerns the  $\hbar \rightarrow 0$  asymptotics of the non-perturbative effects for the ground state and the low-lying states in these potentials. The first phase, which we will call the *strong coupling phase*, is qualitatively and quantitatively very similar to conventional quantum mechanics: tunneling is never suppressed and is mediated by instantons. However, in the so-called *weak coupling phase* we have a very different behavior: instantons become complex and they can interfere destructively, just as in the spin models of [7, 8]. This leads to tunneling suppression at special points, in agreement with the picture developed in [10]. There is a critical point separating the two phases, in which the typical non-perturbative effects induced by tunneling (energy gap and imaginary part of the energy) have an “anomalous” scaling with  $\hbar$ , which we determine analytically.

As we mentioned before, one fascinating aspect of the deformed quantum-mechanical models is that its properties reflect the rich physics of SW theory. It turns out that the existence of two different phases can be understood as a consequence of wall-crossing in the BPS spectrum as we go from strong coupling to weak coupling in the SW moduli space (this is actually the origin of the names we have given to the phases). In addition, the structure of quantum-mechanical instantons corresponds to the spectrum of BPS states in each phase. In particular, we cannot obtain the

correct non-perturbative effects in the weak-coupling phase by a simple analytic continuation of the conventional instantons in the strong coupling phase: we need the new Stokes constants, or BPS invariants, associated to the weak coupling phase. We confirm this with a resurgent analysis of the perturbative series for the ground state energies in both the double-well and the cubic potential. The critical point separating the phases is nothing but a monopole point in the SW moduli space [12, 16], where  $N - 1$  monopoles become massless simultaneously, and where wall-crossing takes place.

The paper is organized as follows. In section 2 we review the basic ingredients of the deformed quantum-mechanical models introduced in [10]. In section 3 we study the strong coupling phase, which from the point of view of quantum mechanics corresponds to not too deep potential wells. We generalize the standard instanton analysis to the deformed case and we compute the non-perturbative effects at one-loop. We also show how this result follows from a WKB-like approach and we test our result against explicit numerical computations of the spectrum. In section 4 we study the weak coupling phase. We show that instantons become complex and acquire a phase that leads to tunneling suppression, and we note that the naive analytic continuation of the conventional instantons fails in the case of the cubic well. We then explain in detail how a resurgent analysis of the perturbative series allows one to obtain the correct instanton structure. In section 5 we analyze the theory at the critical point, and we find that the non-perturbative amplitudes display an “anomalous” scaling with  $\hbar$ , which can however be understood in detail with the help of the all-orders WKB method. Finally, in section 6 we conclude and list some open problems.

## 2 Deformed quantum mechanics

The deformed quantum mechanical model we will consider was introduced and studied in [10]. It is defined by a quantum Hamiltonian of the form

$$H_N = \Lambda^N (e^{\mathbf{p}} + e^{-\mathbf{p}}) + V_N(\mathbf{x}), \quad (2.1)$$

where

$$V_N(x) = \sum_{k=0}^N c_k x^{N-k} \quad (2.2)$$

is a degree  $N$  polynomial, and  $\mathbf{x}, \mathbf{p}$  are the usual Heisenberg operators in  $L^2(\mathbb{R})$ , with

$$[\mathbf{x}, \mathbf{p}] = i\hbar. \quad (2.3)$$

The kinetic term of the Hamiltonian is a deformation of the usual non-relativistic case  $\mathbf{p}^2/2$ . The analogue of the Schrödinger equation is the finite difference equation

$$\Lambda^N (\psi(x + i\hbar) + \psi(x - i\hbar)) + V_N(x)\psi(x) = E\psi(x). \quad (2.4)$$

It is sometimes useful to put together the potential and the energy in a single function,

$$W_N(x) = V_N(x) - E = \sum_{k=0}^N (-1)^k h_k x^{N-k}. \quad (2.5)$$

Finite-difference equations of the form (2.4) have been investigated for a long time. A WKB approach to solve them was put forward by Dingle and Morgan in [17] in the 1960s. More recently

they have received a lot of attention, since they are related to the quantization of mirror curves and of the SW curves of  $\mathcal{N} = 2$  supersymmetric theories. In particular, the Hamiltonian (2.1) was introduced in [10] as a direct quantization of the SW curve of  $SU(N)$ ,  $\mathcal{N} = 2$  Yang–Mills theory [12, 18]. Most of the recent approaches to finite-difference equations are based on the WKB method and its resurgent upgradings, see e.g. [19–21].

The approach of [10] does not rely on the WKB method and is based on the so-called TS/ST correspondence [13, 14] (see e.g. [22] for a review and references). The first aspect of this approach is to regard  $H_N$  as an actual operator on  $L^2(\mathbb{R})$  and study its properties and spectrum. It is easy to see heuristically, or even numerically, that, when  $N$  is even, the operator  $H_N^{-1}$  is trace class, therefore  $H_N$  has a discrete spectrum of energy levels. This has been proved rigorously in [23], building on similar results for the quantization of mirror curves in [24]. Although there are no rigorous results when  $N$  is odd, numerical results indicate that in this case the Hamiltonian  $H_N$  has a discrete spectrum of resonances, akin to what is found in conventional quantum mechanics with odd polynomial potentials (see e.g. [2]).

Once the spectral problem is well-defined, one can ask whether it can be solved by explicit EQCs. The main result of [10] was to obtain such conditions as a limiting, simpler case of the more general EQCs of [13–15]. It turns out that the EQCs for deformed quantum mechanics can be expressed in terms of the so-called Nekrasov–Shatashvili (NS) limit [25] of instanton partition functions [26, 27]. The Hamiltonian  $H_N$  is also closely related to the  $Q$ -operator of the periodic Toda lattice [28]. The function  $W_N(x)$  in (2.5) can be regarded as a generating function of the conserved Hamiltonians  $h_i$  of this integrable system,  $i = 1, \dots, N$  (the value of  $h_0$  sets the overall normalization and one usually sets  $h_{N-1} = 0$ ). The quantum Toda lattice is characterized by a set of eigenvalues  $h_i^T$ ,  $i = 1, \dots, N$ , for these Hamiltonians. By using the EQCs of [10], as well as the EQCs for the Toda lattice conjectured in [25] and proved in [29], one can show the following [10]: when the parameters in the potential  $V_N(x)$  of the Hamiltonian (2.1) take the values corresponding to the Toda lattice eigenvalues,  $h_i^T$ ,  $i = 1, \dots, N - 1$ , the energy  $E$  is determined by the value of  $h_N^T$ . In other words, the Toda lattice eigenvalues are special solutions of the spectral problem of the Hamiltonian  $H_N$ . For this reason, we will call these values of the parameters and the energy the *Toda lattice points*. Note that, when  $N$  is odd, the resonances must become real at these points. In addition, when  $V_4(x)$  has the form of a double-well potential,

$$V_4(x) = h_0 x^4 + h_2 x^2 + h_4, \quad (2.6)$$

one can show that some of the energy levels become degenerate at the Toda lattice points. This suggests that quantum tunneling is *suppressed* at those points, in both of its typical manifestations: as a mechanism to lift the degeneracy of the spectrum in the double-well potential, and as a mechanism for the decay of metastable states.

In this paper we would like to gain a better understanding of this suppression of quantum tunneling. To do that, we will use instantons, which have become standard tools to explain tunneling and to calculate its effects quantitatively. Before addressing this issue in the next section, let us fix our conventions and state some additional results.

We will set  $\Lambda^N = 1/2$ , and include an additional constant  $-1$  in the potential  $V_N(x)$ , so that the Hamiltonian will read

$$H_N = \cosh(\mathbf{p}) - 1 + u_N(x). \quad (2.7)$$

This normalization is chosen in such a way that, for  $p$  small, one recovers the standard non-relativistic kinetic term  $p^2/2$ . We will focus on two cases for the potential: the double-well potential for  $N = 4$ , and the cubic potential for  $N = 3$ . The double-well potential will be

parametrized as

$$u_4(x) = \frac{1}{2} \left( x^2 - \frac{h}{2} \right)^2, \quad h > 0. \quad (2.8)$$

We have chosen the constant term so as to have zero classical energy at the equilibrium points  $x = \pm x_*$ , with

$$x_* = \sqrt{\frac{h}{2}}. \quad (2.9)$$

In terms of the parameters in  $W_4(x)$  we have

$$h_2 = -\frac{h}{2}, \quad h_4 = -1 + \frac{h^2}{8} - E. \quad (2.10)$$

The cubic potential is taken to be

$$u_3(x) = \frac{1}{2} \left( x^3 - hx + \frac{2hx_*}{3} \right), \quad x_* = \sqrt{\frac{h}{3}}, \quad h > 0, \quad (2.11)$$

so that we also have zero energy at the minimum at  $x_*$ . The parameters in  $W_3(x)$  are

$$h_2 = -\frac{h}{2}, \quad h_3 = -1 + \left( \frac{h}{3} \right)^{3/2} - E. \quad (2.12)$$

With our normalization, the parameter  $h$  in the above potentials coincides with the one used in the quartic and cubic potentials in [10] when  $\Lambda = 1$ .

Let us note that the classical EOM for the Hamiltonian (2.7) are

$$\dot{x} = \sinh(p), \quad \dot{p} = -u'(x), \quad (2.13)$$

so that motion at constant energy  $E$  is determined by the equation

$$\sqrt{1 + \dot{x}^2} - 1 + u(x) = E. \quad (2.14)$$

This implies that regions where  $u(x) > E$  are classically forbidden, as in conventional classical mechanics (when specifying  $N$  is not necessary, we will write  $u(x)$  instead of  $u_N(x)$ ).

### 3 Strong coupling phase

#### 3.1 Nonperturbative effects from instantons

Let us now study instanton configurations in this theory. Recall that, in standard quantum mechanics, instantons are responsible for two important phenomena, as mentioned in the previous section.

The first phenomenon is lifting the degeneracy of the spectrum in the double-well potential. This energy spectrum has naively a double degeneracy at each energy level in perturbation theory. This degeneracy is broken by quantum tunneling, and there is a non-perturbatively small difference between  $E_{2k}$  and  $E_{2k+1}$  for  $k = 0, 1, \dots$ , where  $E_{2k}$  and  $E_{2k+1}$  correspond respectively to parity even and parity odd wavefunctions. To detect this small energy difference at the lowest level, we consider the thermal partition function with anti-periodic boundary conditions [30]

$$Z_a(\beta) = \text{Tr} \mathbf{P} e^{-\beta \mathbf{H}/\hbar} = e^{-\beta E_0/\hbar} - e^{-\beta E_1/\hbar} + \dots, \quad (3.1)$$

where  $P$  is the parity operator. In the semi-classical limit, it is dominated by

$$Z_a(\beta) \approx e^{-\beta E_0/\hbar} \frac{\beta}{\hbar} \Delta E + \dots \quad (3.2)$$

where

$$\Delta E = E_1 - E_0 \quad (3.3)$$

is the energy gap between the ground state and the first excited state. We also define the thermal partition function with periodic boundary conditions,

$$Z_p(\beta) = \text{Tr} e^{-\beta H/\hbar} = e^{-\beta E_0/\hbar} + \dots, \quad (3.4)$$

which in the semi-classical limit is dominated by the ground state energy. We can express the energy gap  $\Delta E$  by

$$\Delta E = \lim_{\beta \rightarrow \infty} \frac{\hbar Z_a(\beta)}{\beta Z_p(\beta)}. \quad (3.5)$$

Both  $Z_p(\beta)$  and  $Z_a(\beta)$  can be computed by Euclidean path integrals as follows,

$$Z(\beta) = \int \mathcal{D}x(\tau) \mathcal{D}p(\tau) \exp \left[ -\frac{1}{\hbar} \int_{-\beta/2}^{+\beta/2} d\tau (H(x, p) - i\dot{x}p) \right] \quad (3.6)$$

with respectively periodic and anti-periodic boundary conditions. In the semi-classical limit,  $Z_p$  is dominated by the contribution from the stationary saddle configuration, which we denote by  $Z_0$ , while  $Z_a$  is dominated by the contribution from the instanton saddle configuration with anti-periodic boundary conditions, which we denote by  $Z_1^{(-)}$ . Therefore (3.5) can also be written as

$$\Delta E = \lim_{\beta \rightarrow \infty} \frac{\hbar Z_1^{(-)}(\beta)}{\beta Z_0(\beta)}. \quad (3.7)$$

The second phenomenon is the decay of metastable states in the cubic potential. The cubic potential has a discrete spectrum of resonances which can be obtained by imposing the Gamow-Siegert boundary condition. The complex energies of these resonant states have non-perturbatively small negative imaginary parts which characterize their decay rate. To detect this small imaginary part at the lowest level, we consider again the thermal partition function with periodic boundary conditions,

$$Z(\beta) = \text{Tr} e^{-\beta H/\hbar} = e^{-\beta E_0/\hbar} + \dots \quad (3.8)$$

This partition function also has a small imaginary part, just like the energies. In the semi-classical limit, it is dominated by the ground state energy, and

$$E_0 = - \lim_{\beta \rightarrow \infty} \frac{\hbar}{\beta} \log Z(\beta) \quad (3.9)$$

By splitting both  $E_0$  and  $Z(\beta)$  into a real part and a imaginary part, one finds that

$$\text{Im} E_0 = - \lim_{\beta \rightarrow \infty} \frac{\hbar \text{Im} Z(\beta)}{\beta \text{Re} Z(\beta)}. \quad (3.10)$$

On the other hand, the partition function  $Z(\beta)$  is also given by a path integral formula (3.6) with periodic boundary condition. In the semi-classical limit, it is dominated by the stationary configuration, and

$$\operatorname{Re} Z(\beta) \approx \operatorname{Re} Z_0(\beta). \quad (3.11)$$

To find the main contribution to  $\operatorname{Im} Z(\beta)$ , one notices that the partition function, as a function of  $\hbar$ , has a branch cut across the positive real axis, and the discontinuity

$$Z(\hbar + i0, \beta) - Z(\hbar - i0, \beta) = 2i \operatorname{Im} Z(\hbar, \beta) \quad (3.12)$$

is given at leading order by the contribution from the instanton configuration, which we denote by  $Z_1^{(+)}(\beta)$ . Therefore,

$$\operatorname{Im} E_0 = - \lim_{\beta \rightarrow \infty} \frac{\hbar}{2\beta} \frac{\operatorname{Im} Z_1^{(+)}(\beta)}{\operatorname{Re} Z_0(\beta)}, \quad (3.13)$$

see [4, 5] for a recent detailed derivation of this formula, and an illuminating discussion of the relation between resonances and instanton calculus.

To summarize, both the lifting of the ground state energy degeneracy and the decay of the metastable ground state are characterized by the quantity

$$R(\hbar) := \lim_{\beta \rightarrow \infty} \frac{\hbar}{\beta} \frac{Z_1(\beta)}{Z_0(\beta)}, \quad (3.14)$$

where  $Z_1(\beta)$  is the contribution to the thermal partition function from the instanton configuration with either periodic or anti-periodic boundary condition, and  $Z_0(\beta)$  is the contribution from the stationary configuration. These considerations should apply as well to deformed quantum mechanics, where the kinetic term in the Hamiltonian is  $\cosh(p) - 1$  instead of  $p^2/2$  as in (2.7). We will now verify this in detail.

### 3.2 Instanton contribution in deformed quantum mechanics

Let us consider a generic deformed quantum mechanical model with the Hamiltonian

$$H(x, p) = \cosh(p) - 1 + u(x). \quad (3.15)$$

We also assume that the potential  $u(x)$  has a preferred local minimum  $x_*$  where the potential vanishes, i.e.

$$u(x) \approx \frac{\omega^2}{2} (x - x_*)^2 + \mathcal{O}((x - x_*)^3). \quad (3.16)$$

In this equation,  $\omega$  is the circular frequency. For instance,

- the double-well potential (2.8) has two local minima and we can choose  $x_* = \sqrt{\hbar/2}$  to be the preferred one where  $\omega = \sqrt{2\hbar}$ ;
- the cubic potential (2.11) has a preferred local minimum at  $x_* = \sqrt{\hbar/3}$  where  $\omega = (3\hbar)^{1/4}$ .

We are interested in the thermal partition function

$$Z(\beta) = \int \mathcal{D}x(\tau) \mathcal{D}p(\tau) \exp \left[ -\frac{1}{\hbar} \int_{-\beta/2}^{\beta/2} d\tau (H(x, p) - i\dot{x}p) \right] \quad (3.17)$$



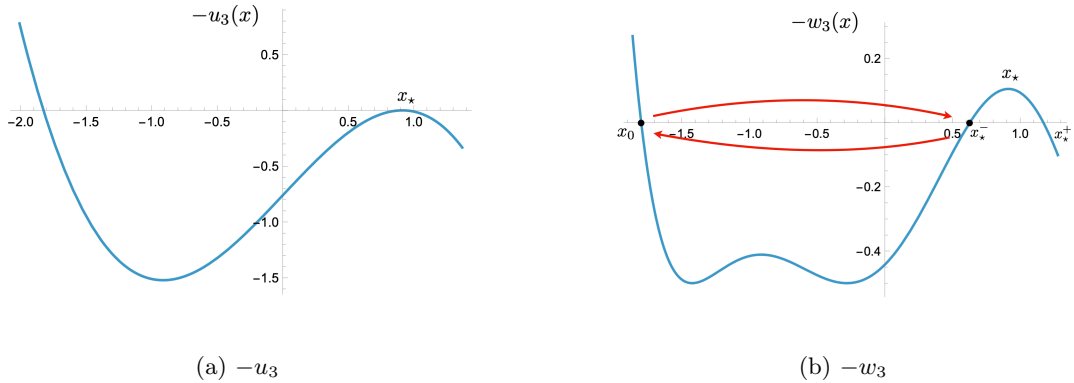


**Figure 2:** The inverted potentials  $-u_3(x)$  and  $-w_3(x)$  of the cubic model, with  $h = 2.5$  and  $E = -0.1$ . In the plot of  $-w_3(x)$  we also indicate the trajectory of the instanton configuration.

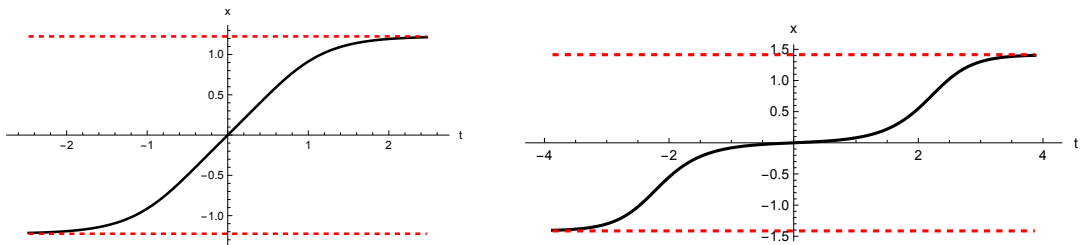


**Figure 3:** The trajectories of the instanton  $x(\tau)$  in the double well, for  $\tau = x_0 = 0$  and  $E = 0$ . The figure on the left is for  $h = 3$ , while the figure on the right is for  $h = 3.999$ . The horizontal lines denote the asymptotic values  $\mp x_*$ .

1-instanton configuration. The inverted potential  $-w(x)$  has a potential well next to the local maximum  $x_*$ . The instanton configuration has negative energy  $E$  and is bounded inside the potential well, with two turning points. One of the turning points is the solution of  $w(x; E) = 0$  which is near the local maximum  $x_*$  and inside the potential well. We will denote it by  $x_*^-$ . There are then two different cases

- In the case of the double-well potential, the instanton configuration starts at the turning point  $x_*^-$ , and arrives at the opposite turning point in the potential well after a time  $\beta$ , as shown in Fig. 1. It satisfies anti-periodic boundary conditions. Note that due to the parity of the potential, there is also anti-instanton solution whose trajectory is flipped horizontally.
- In the case of the cubic potential, the instanton configuration starts from the turning point  $x_*^-$ , bounces off the opposite turning point in the potential well, and returns to  $x_*^-$  after a time  $\beta$ , as shown in Fig. 2. It satisfies periodic boundary conditions.

In both cases, we can solve (3.20) to obtain  $\tau(x)$  as a function of  $x$ ,

$$\tau - \tau_0 = \int_{x_0}^x \frac{dx'}{\sqrt{(E + u(x'))(2 - E - u(x'))}}. \quad (3.24)$$

The instanton configuration has a free parameter or collective coordinate: the time  $\tau_0$ . At this time, the instanton is located at certain position  $x_0$ , that will be called the center of the instanton

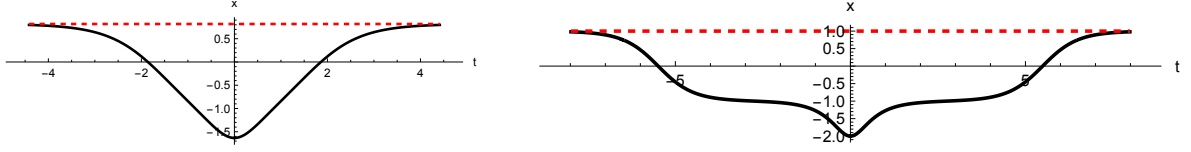


**Figure 4:** The trajectories of the instanton  $x(\tau)$  in the cubic potential, for  $\tau = 0$ ,  $x_0$  the turning point, and  $E = 0$ . The figure on the left is for  $h = 2$ , while the figure on the right is for  $h = 2.999$ . The horizontal line is  $x_*$ .

and that we will choose conveniently. The instanton trajectories when  $E = 0$  can be calculated explicitly from (3.24) (the integral can be computed in terms of elliptic functions), and we show them in Fig. 3 and Fig. 4 for the double well and the cubic potential, respectively, and two different values of  $h$ . For small values of  $h$ , these profiles are very similar to the ones found in conventional quantum mechanics, but as we approach the values  $h = 4$  for the double well and  $h = 3$  for the cubic potential, the profiles get deformed and seem to split into pieces. We will come back to this at the end of this section.

Let us consider the contributions of these two saddle configurations to the path integral. First, we consider the stationary solution which sits at the preferred local maximum  $x = x_*$  of the inverted potential. To find its contribution to the path integral, we expand the Hamiltonian near the stationary solution through

$$x = x_* + \delta x, \quad p = \delta p, \quad (3.25)$$

and obtain

$$H(x, p) = \delta p^2 + \frac{1}{2}\omega^2\delta x^2. \quad (3.26)$$

Its contribution to the partition function reads

$$Z_0(\beta) \approx \int \mathcal{D}\delta x \mathcal{D}\delta p \exp \left[ -\frac{1}{\hbar} \int_{-\beta/2}^{+\beta/2} d\tau \left( \frac{1}{2}\delta p^2 + \frac{1}{2}\omega^2\delta x^2 - i\delta\dot{x}\delta p \right) \right]. \quad (3.27)$$

After integrating over  $\delta p$ , we obtain

$$Z_0(\beta) \approx \int \mathcal{D}\delta x \exp \left[ -\frac{1}{\hbar} \int_{-\beta/2}^{+\beta/2} d\tau \left( \frac{1}{2}\delta\dot{x}^2 + \frac{1}{2}\omega^2\delta x^2 \right) \right] \quad (3.28)$$

$$= \frac{1}{\sqrt{\det \mathbf{O}_0}} \quad (3.29)$$

where  $\mathbf{O}_0$  is the operator

$$\mathbf{O}_0 = -\frac{\partial^2}{\partial\tau^2} + \omega^2. \quad (3.30)$$

Next, we consider the contribution of the instanton configuration, which we will denote by  $x_1(\tau)$  together with  $p_1(\tau)$ . Expanding near the instanton configuration,

$$x = x_1 + \delta x, \quad p = p_1 + \delta p, \quad (3.31)$$

we find

$$Z_1(\beta) = e^{-S/\hbar} \int \mathcal{D}\delta x \exp \left[ -\frac{1}{2\hbar} \int_{-\beta/2}^{\beta/2} d\tau \delta x \tilde{\mathbf{O}}_1 \delta x \right] \quad (3.32)$$

where  $\mathcal{S}$  is the action of the instanton configuration

$$\mathcal{S} = \int_{-\beta/2}^{\beta/2} d\tau (H(x, p) - i\dot{x}p), \quad (3.33)$$

and

$$\tilde{\mathcal{O}}_1 = -\sqrt{\cosh p_1} \partial_\tau \frac{1}{\cosh p_1} \partial_\tau \sqrt{\cosh p_1} + u''(x_1) \cosh p_1. \quad (3.34)$$

The operator  $\tilde{\mathcal{O}}_1$  has a zero mode (implicitly depending on  $\tau_0$ )

$$\frac{\dot{x}_1(\tau)}{\sqrt{\cosh p_1(\tau)}}, \quad (3.35)$$

and after integrating over the zero mode separately, we obtain (see e.g. [3] for a detailed derivation)

$$Z_1(\beta) = \frac{\beta \mathcal{W}(E)^{1/2}}{\sqrt{2\pi\hbar}} \frac{e^{-\mathcal{S}/\hbar}}{\sqrt{\det' \tilde{\mathcal{O}}_1}}. \quad (3.36)$$

where

$$\mathcal{W}(E) = \int_{-\beta/2}^{\beta/2} d\tau \frac{\dot{x}_1(\tau)^2}{\cosh p_1(\tau)}, \quad (3.37)$$

and  $\det' \tilde{\mathcal{O}}_1$  is the determinant of the operator  $\tilde{\mathcal{O}}_1$  once the zero mode has been removed.

To evaluate the functional determinants (3.29) and (3.36), we apply the Gel'fand-Yaglom theorem (see e.g. [2, 3, 31] for an exposition). Let  $\psi_{1,2}$  be two wavefunctions annihilated by the operator

$$\mathcal{O} = -\partial_t^2 + \dots \quad (3.38)$$

with the boundary conditions

$$\begin{aligned} \psi_1(-\beta/2) &= 1, & \dot{\psi}_1(-\beta/2) &= 0, \\ \psi_2(-\beta/2) &= 0, & \dot{\psi}_2(-\beta/2) &= 1. \end{aligned} \quad (3.39)$$

Then,

$$\det \mathcal{O} = \text{Tr} \left[ \begin{pmatrix} \psi_1(\beta/2) & \dot{\psi}_1(\beta/2) \\ \psi_2(\beta/2) & \dot{\psi}_2(\beta/2) \end{pmatrix} \mp \mathbf{1} \right] = \psi_1(\beta/2) + \dot{\psi}_2(\beta/2) \mp 2, \quad (3.40)$$

where  $\mp$  correspond respectively to periodic and anti-periodic boundary conditions of the wavefunctions in the domain of the operators.

For the operator of the stationary configuration (3.30), the two solutions can be chosen to be

$$\psi_1(\tau) = \cosh \omega(\tau + \beta/2), \quad \psi_2(\tau) = \omega^{-1} \sinh \omega(\tau + \beta/2). \quad (3.41)$$

Therefore, the determinant is

$$\det \mathcal{O}_0 = 2 \cosh \omega\beta - 2 = 4 \sinh^2 \omega\beta/2, \quad (3.42)$$

where we have used that the stationary configuration satisfies periodic boundary conditions.

To calculate the determinant of the operator of the instanton configuration (3.34), we use the trick that, for an operator that only has one zero mode, we have [3]

$$\det' \mathcal{O} = \lim_{\lambda \rightarrow 0} \frac{d}{d\lambda} \det \mathcal{O}_\lambda, \quad (3.43)$$

where  $\mathbf{O}_\lambda$  is the perturbed operator

$$\mathbf{O}_\lambda = \mathbf{O} + \lambda. \quad (3.44)$$

The primed determinant in Eq. (3.43) can be also calculated by using the Gel'fand-Yaglom theorem. We consider  $\lambda$ -dependent wavefunctions, annihilated by the perturbed operator  $\mathbf{O}_\lambda$ , and we expand them as

$$\psi_{j,\lambda} = \psi_j^{(0)} + \lambda\psi_j^{(1)} + \dots \quad (3.45)$$

By solving in power series in  $\lambda$ , we find that the components must satisfy the following equations

$$\mathbf{O}\psi_j^{(0)} = 0, \quad (3.46a)$$

$$\mathbf{O}\psi_j^{(1)} = -\dot{\psi}_j^{(0)}. \quad (3.46b)$$

Furthermore, the boundary conditions (3.39) indicate that  $\psi_j^{(0)}, \psi_j^{(1)}$  must obey the following individual boundary conditions

$$\psi_1^{(0)}(-\beta/2) = 1, \quad \dot{\psi}_1^{(0)}(-\beta/2) = 0, \quad (3.47a)$$

$$\psi_2^{(0)}(-\beta/2) = 0, \quad \dot{\psi}_2^{(0)}(-\beta/2) = 1, \quad (3.47b)$$

as well as

$$\psi_1^{(1)}(-\beta/2) = 0, \quad \dot{\psi}_1^{(1)}(-\beta/2) = 0, \quad (3.48a)$$

$$\psi_2^{(1)}(-\beta/2) = 0, \quad \dot{\psi}_2^{(1)}(-\beta/2) = 0. \quad (3.48b)$$

In terms of these components, it is easy to see that the primed determinant of  $\mathbf{O}$  is

$$\det' \mathbf{O} = \psi_1^{(1)}(\beta/2) + \dot{\psi}_2^{(1)}(\beta/2). \quad (3.49)$$

Note that this result holds true for both periodic and anti-periodic boundary conditions.

In the case of (3.34), we can use the property of the determinant

$$\det(\mathbf{O} + \lambda) = \det(f \cdot \mathbf{O} \cdot f^{-1} + \lambda), \quad (3.50)$$

to change the normalization of the operator and find

$$\det' \tilde{\mathbf{O}}_1 = \det' \mathbf{O}_1 = \lim_{\lambda \rightarrow 0} \frac{d}{d\lambda} \det \mathbf{O}_{1,\lambda} \quad (3.51)$$

where

$$\mathbf{O}_{1,\lambda} = \mathbf{O}_1 + \lambda, \quad (3.52)$$

and

$$\begin{aligned} \mathbf{O}_1 &= \cosh p_1 \left( -\partial_\tau \frac{1}{\cosh p_1} \partial_\tau + u''(x_1) \right) \\ &= -\frac{\partial^2}{\partial \tau^2} + (\partial_\tau \log \cosh p_1) \frac{\partial}{\partial \tau} + \cosh p_1 u''(x_1). \end{aligned} \quad (3.53)$$

We then proceed as follows: we first find the two solutions  $\psi_j^{(0)}$  annihilated by the operator  $\mathbf{O}_1$ . It is already known from (3.35) that  $\dot{x}_1(\tau)$  is annihilated by  $\mathbf{O}_1$ , and is in fact a zero mode as it satisfies the required periodic or anti-periodic boundary conditions. It depends implicitly on a free parameter  $\tau_0$ , and by choosing it appropriately we can demand

$$\ddot{x}_1(-\beta/2) = 0, \quad (3.54)$$

which holds e.g. if at  $\tau = -\beta/2$  the particle sits at the local minimum of the inverted potential. We can then choose  $\psi_1^{(0)}$  to be

$$\psi_1^{(0)}(\tau) = \frac{\dot{x}_1(\tau)}{\dot{x}_1(-\beta/2)}, \quad (3.55)$$

so that it satisfies the boundary condition (3.47a). In addition, as argued in [3, Sec. 1.6],

$$\chi(\tau) = \frac{\partial x_1(\tau; E)}{\partial E} \quad (3.56)$$

is also annihilated by  $\mathbf{O}_1$ , but it satisfies neither the periodic nor the anti-periodic boundary conditions. In fact, by taking a derivative with respect to  $E$  on both sides of (3.20), we find

$$\dot{x}_1(\tau)\dot{\chi}(\tau) - \ddot{x}_1(\tau)\chi(\tau) = \cosh p_1(\tau). \quad (3.57)$$

Because of the simplifying assumption (3.54) we have made, (3.57) implies that

$$\dot{x}_1(-\beta/2)\dot{\chi}_1(-\beta/2) = \cosh p_1(-\beta/2). \quad (3.58)$$

Therefore, we can choose  $\psi_2^{(0)}$  to be

$$\psi_2^{(0)}(\tau) = \frac{\chi(\tau)\dot{x}_1(-\beta/2) - \dot{x}_1(\tau)\chi(-\beta/2)}{\cosh p_1(-\beta/2)}, \quad (3.59)$$

so that it satisfies the boundary conditions (3.48b). Note that  $\psi_j^{(0)}(\tau)$  in addition satisfy another set of boundary conditions

$$\psi_1^{(0)}(\beta/2) = \dot{\psi}_2^{(0)}(\beta/2) = \pm 1, \quad \dot{\psi}_1^{(0)}(\beta/2) = 0, \quad (3.60)$$

thanks to the periodic or anti-periodic boundary conditions of  $x_1(\tau)$ .

Next, we propose that  $\psi_j^{(1)}$  can be constructed as

$$\psi_j^{(1)}(\tau) = \cosh p_1(-\beta/2) \int_{-\beta/2}^{\tau} d\tau' \frac{\psi_j^{(0)}(\tau')}{\cosh p_1(\tau')} \left( \psi_2^{(0)}(\tau)\psi_1^{(0)}(\tau') - \psi_1^{(0)}(\tau)\psi_2^{(0)}(\tau') \right). \quad (3.61)$$

We find that the Wronskian of the solutions  $\psi_j^{(0)}$  to the differential operator (3.53) is

$$W(\tau) = \psi_1^{(0)}(\tau)\dot{\psi}_2^{(0)}(\tau) - \psi_2^{(0)}(\tau)\dot{\psi}_1^{(0)}(\tau) = \frac{\cosh p_1(\tau)}{\cosh p_1(-\beta/2)}. \quad (3.62)$$

By using the Wronskian relation, one can easily check that (3.61) indeed satisfies the second equation of (3.46) as well as the boundary conditions (3.48). Plugging (3.61) into (3.49) we get

$$\begin{aligned} \det' \mathbf{O}_1 = \cosh p_1(-\beta/2) & \left[ \psi_2^{(0)}(\beta/2) \int_{-\beta/2}^{\beta/2} d\tau \frac{\psi_1^{(0)}(\tau)^2}{\cosh p_1(\tau)} - \dot{\psi}_1^{(0)}(\beta/2) \int_{-\beta/2}^{\beta/2} d\tau \frac{\psi_2^{(0)}(\tau)^2}{\cosh p_1(\tau)} \right. \\ & \left. + \left( \dot{\psi}_2^{(0)}(\beta/2) - \psi_1^{(0)}(\beta/2) \right) \int_{-\beta/2}^{\beta/2} d\tau \frac{\psi_1^{(0)}(\tau)\psi_2^{(0)}(\tau)}{\cosh p_1(\tau)} \right]. \end{aligned} \quad (3.63)$$

Using the boundary conditions (3.60), it can be written as

$$\det' \mathbf{O}_1 = \frac{\chi(\beta/2) \mp \chi(-\beta/2)}{\dot{x}_1(-\beta/2)} \int_{-\beta/2}^{\beta/2} d\tau \frac{\dot{x}_1(\tau)^2}{\cosh p_1(\tau)}. \quad (3.64)$$

Furthermore, taking derivatives with respect to  $E$  on the periodic/anti-periodic boundary condition

$$x_1(\tau + \beta; E) = \pm x_1(\tau; E) \quad (3.65)$$

we find

$$\frac{\chi(\beta/2) \mp \chi(-\beta/2)}{\dot{x}_1(-\beta/2)} = \mp \frac{\partial \beta}{\partial E}, \quad (3.66)$$

which allows us to further simplify (3.64)

$$\det' \mathbf{O}_1 = \mp \left( \frac{\partial E}{\partial \beta} \right)^{-1} \mathcal{W}(E), \quad (3.67)$$

where we have also used (3.37). Let us note that (3.67) is the same result that one obtains in conventional quantum mechanics. The only difference is that the period  $\beta$  is computed by a different period integral.

Putting together (3.29), (3.42), (3.36) and (3.67), we conclude that

$$\frac{Z_1(\beta)}{Z_0(\beta)} = \frac{\beta(\mathcal{W}(E))^{1/2}}{\sqrt{2\pi\hbar}} \sqrt{\frac{\det \mathbf{O}_0}{\det' \tilde{\mathbf{O}}_1}} e^{-\mathcal{S}/\hbar} = \frac{2\beta \sinh(\omega\beta/2)}{\sqrt{\mp 2\pi\hbar}} \left( \frac{\partial E}{\partial \beta} \right)^{1/2} e^{-\mathcal{S}/\hbar}, \quad (3.68)$$

where in the denominator the sign  $\mp$  correspond to periodic and anti-periodic boundary conditions for  $Z_1$ , respectively.

To proceed further, we will calculate  $\partial E/\partial \beta$ . We also note that we have to take the limit  $\beta \rightarrow \infty$ , which, as in standard instanton calculus, corresponds to  $E \rightarrow 0$ . By definition,

$$\beta(E) = \oint d\tau = \oint \frac{dx}{\dot{x}} = 2 \int_{x_0(E)}^{x_\star^-(E)} \frac{dx}{\sqrt{(E + u(x))(2 - E - u(x))}}. \quad (3.69)$$

In the last step, we used the EOM (3.20).  $x_0(E)$  is the centre of the instanton configuration, we can choose it to be 0 for the double-well potential (see Fig. 1) and the other turning point for the cubic potential (see Fig. 2). Note that this integral is singular in the limit  $E \rightarrow 0$  we are interested in. The function inside the square root factorizes as

$$(E + u(x))(2 - E - u(x)) = (x - x_\star^-(E))(x - x_\star^+(E))p(x; E), \quad (3.70)$$

where  $x_\star^\pm(E)$  are the two zeros of  $u(x) + E$  near the local maximum  $x_\star$ . In the limit  $E \rightarrow 0$

$$x_\star^\pm(E) \rightarrow x_\star, \quad (3.71)$$

and the integral becomes

$$\beta(E) \approx 2 \int^{x_\star} \frac{dx}{(x_\star - x)\sqrt{p(x; 0)}} \quad (3.72)$$

which is divergent. To regularize this divergence, we write

$$\begin{aligned}
(\omega/2)\beta(E) &= \int_{x_0(E)}^{x_\star^-(E)} \frac{\omega dx}{\sqrt{(E+u(x))(2-E-u(x))}} - \int_{x_0(E)}^{x_\star^-(E)} \frac{dx}{\sqrt{(x-x_\star^-(E))(x-x_\star^+(E))}} \\
&+ \int_{x_0(E)}^{x_\star^-(E)} \frac{dx}{\sqrt{(x-x_\star^-(E))(x-x_\star^+(E))}}.
\end{aligned} \tag{3.73}$$

The first line is now regular as  $E \rightarrow 0$ , and up to  $\mathcal{O}(E)$  it is given by

$$\mathcal{A} = \int_{x_0}^{x_\star} \frac{\omega dx}{\sqrt{u(x)(2-u(x))}} - \int_{x_0}^{x_\star} \frac{dx}{x_\star - x}, \tag{3.74}$$

where  $x_0 = x_0(E=0)$ . The second line is

$$\log \frac{\sqrt{x_\star^+(E) - x_0(E)} + \sqrt{x_\star^-(E) - x_0(E)}}{\sqrt{x_\star^+(E) - x_0(E)} - \sqrt{x_\star^-(E) - x_0(E)}} \approx -\frac{1}{2} \log(-E) + \log\left(\sqrt{2}\omega(x_\star - x_0)\right) + \mathcal{O}(E). \tag{3.75}$$

Solving  $E$  from  $\beta$ , we arrive at

$$\frac{\partial E}{\partial \beta} \approx 2\omega^3(x_\star - x_0)^2 e^{-\omega\beta + 2\mathcal{A}} \tag{3.76}$$

as  $\beta \rightarrow \infty$ . Plugging this into (3.68), we finally conclude that  $R(\hbar)$ , defined by (3.14), evaluates to

$$R^{(\pm)}(\hbar) = \sqrt{\frac{\hbar}{\mp\pi}} \omega^{3/2} (x_\star - x_0) e^{-\mathcal{S}/\hbar + \mathcal{A}}, \tag{3.77}$$

where the sign  $\mp$  in the denominator corresponds to the periodic and anti-periodic boundary conditions respectively, and  $\mathcal{S}$  is the instanton action in the  $\beta \rightarrow \infty$  limit, or equivalently, in the  $E \rightarrow 0$  limit, which is given by

$$\mathcal{S} = \lim_{\beta \rightarrow \infty} \int_{-\beta/2}^{\beta/2} d\tau (H(x, p) - i\dot{x}p) = -i \lim_{\beta \rightarrow \infty} \oint_{\gamma} p dx = -2i \int_{x_0}^{x_\star} \cosh^{-1}(1-u(x)) dx, \tag{3.78}$$

where  $\gamma$  is the trajectory of the instanton configuration. It is also given by

$$\mathcal{S} = 2 \int_{x_0}^{x_\star} \cos^{-1}(1-u(x)) dx. \tag{3.79}$$

We can now write down our final formulae. For the double-well potential we find that the energy gap is given by

$$\Delta E = 2R^{(-)}(\hbar) = 2\sqrt{\frac{\hbar}{\pi}} \omega^{3/2} (x_\star - x_0) e^{-\mathcal{S}/\hbar + \mathcal{A}}, \tag{3.80}$$

with

$$x_0 = 0, \quad x_\star = \sqrt{\hbar/2}, \quad \omega = (2\hbar)^{1/2}. \tag{3.81}$$

In (3.80) we have included an additional factor of 2, which takes into account the contribution of both the instanton and the anti-instanton. We can also write

$$\Delta E = \sqrt{\frac{\hbar}{\pi}} (2h)^{5/4} e^{-\mathcal{S}/\hbar + \mathcal{A}}. \quad (3.82)$$

In the case of the cubic potential, the imaginary part of the ground state energy is given by

$$\text{Im } E = -\frac{1}{2} \text{Im } R^{(+)}(\hbar) = -\frac{1}{2} \sqrt{\frac{\hbar}{\pi}} \omega^{3/2} (x_{\star} - x_0) e^{-\mathcal{S}/\hbar + \mathcal{A}}, \quad (3.83)$$

with

$$x_0 = -2x_{\star}, \quad x_{\star} = \sqrt{\hbar/3}, \quad \omega = (3h)^{1/4}. \quad (3.84)$$

We can also write

$$\text{Im } E = -\sqrt{\frac{\hbar}{\pi}} \frac{(3h)^{7/8}}{2} e^{-\mathcal{S}/\hbar + \mathcal{A}}. \quad (3.85)$$

As expected from (3.64), these formulae are formally identical to the results obtained in conventional quantum mechanics, but the quantities  $\mathcal{S}$  and  $\mathcal{A}$  are periods of different differentials (for example, in standard quantum mechanics,  $\mathcal{S}$  is obtained by integrating the Liouville form  $p(x)dx$ , while here we integrate  $\cosh(p(x))dx$ ).

The results of the instanton analysis presented in this section are not valid for all values of the parameter  $h$  in the potentials (2.8) and (2.11). The reason is that, if  $h$  is sufficiently large, the classical instanton trajectory, given by the integral (3.24) at  $E = 0$ , is no longer real, since the value of  $u(x)$  in the integration interval is greater than 2, and the integral is complex. It is easy to see that the critical values for  $h$  occur at

$$h_c = 3, \quad h_c = 4, \quad (3.86)$$

for the cubic potential and the double-well potential, respectively. For these values,  $u(x)$  has a critical point (a local maximum) at which  $u(x) = 2$ . Similarly, the action of the instanton (3.79), which is real and positive for  $h < h_c$ , becomes complex. An illustration of the shape of the double-well potential at  $h < 4$ ,  $h = 4$  and  $h > 4$  is shown in Fig. 5. As we will see, we can think of this as a *phase transition*, since the asymptotics as  $\hbar \rightarrow 0$  of the non-perturbative effects changes discontinuously as  $h$  varies through its critical value. The behavior at  $h = h_c$  is also special: the scaling with  $\hbar$  becomes “anomalous”, displaying a non-trivial power law, as we will see in detail in section 5. The approach to criticality can be also seen in the instanton trajectories shown in Fig. 3 and Fig. 4. When we are very close to the critical point, they “split” into smaller trajectories. The splitting point is the local maximum at which  $u(x) = 2$ .

We will call the phase  $h < h_c$  the *strong coupling phase*, and the phase with  $h > h_c$  the *weak coupling phase*. This is somewhat counter-intuitive but it is motivated by the following. As we noted in section 2, the parameters in the potential are mapped to the moduli of the SW curve for the  $SU(N)$  theory. It is easy to see that the values (3.86), together with the corresponding values of  $h_{3,4}$  in (2.12), (2.10) with  $E = 0$ , correspond precisely to one of the *monopole points* [12, 16] in the moduli space of the  $SU(3)$ ,  $SU(4)$  SW curve, respectively (the one with real coordinates). These points mark the boundary between the strong coupling and the weak coupling phase of SW theory. There is actually a discontinuous change in SW theory at this point, namely, a jump in the BPS spectrum (or wall-crossing). As we will see in the next section, this jump is the ultimate responsible for the discontinuous asymptotics of the non-perturbative effects in deformed quantum mechanics.

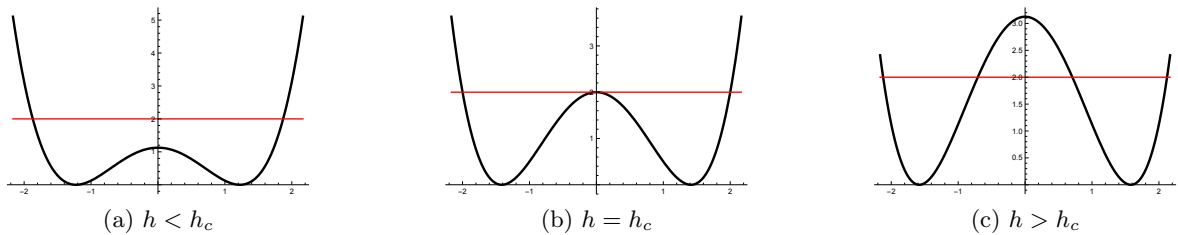


**Figure 5:** As we change the value of the parameter  $h$  in the double well and cubic potentials, the theory undergoes a phase transition at a critical value  $h = h_c$ . Here we show the change in the form of the potential in the case of the double well.

### 3.3 From instantons to WKB

The instanton results derived above are valid only for the ground state energy, since we considered trajectories of classical vanishing energy. In order to obtain results for excited states it is more convenient to use the exact WKB method (see [32] for a recent review). In the case of difference equations, this method has not been developed in enough detail to allow a computation of the EQC, but we can use the instanton results (3.80), (3.83) to obtain an educated guess for all energy levels. Let us first review the situation for the conventional double and cubic wells, following [2].

Let us denote by

$$\Pi_{\text{WKB}}(E; \hbar) = \sum_{\ell \geq 0} \Pi_{\text{WKB}}^{(\ell)}(E) \hbar^{2\ell}, \quad (3.87)$$

the tunneling quantum period appearing in both the cubic and the double-well potentials. Its leading term is

$$\Pi_{\text{WKB}}^{(0)}(E) = 2 \int_{x_0(E)}^{x_*^-(E)} \sqrt{2(V(x) - E)} dx. \quad (3.88)$$

Let us suppose that this is the only non-perturbative period that has to be considered in our problem (as it happens in fact in conventional quantum mechanics). Then, at leading non-perturbative order, we have the following formula for the energy splitting of the  $\nu$ -th energy level in the double-well potential [33]:

$$\Delta E(\nu) \approx \frac{1}{\pi} \frac{\partial E}{\partial \nu} e^{-\Pi_{\text{WKB}}(E; \hbar)/\hbar}. \quad (3.89)$$

Here, in the r.h.s.,  $E = E(\nu; \hbar)$  is the perturbative quantum energy as a function of the shifted quantum number

$$\nu = n + \frac{1}{2}, \quad (3.90)$$

and we have of course

$$E = \hbar\omega\nu + \mathcal{O}(\hbar^2). \quad (3.91)$$

An important subtlety is that, after using (3.91), the higher orders in  $\hbar$  of  $\Pi_{\text{WKB}}/\hbar$  give contributions which are  $\hbar$ -independent and singular at  $\nu = 0$ <sup>1</sup>. They are given by

$$\nu(\log \nu - 1) - \frac{1}{24\nu} + \frac{7}{2880\nu^3} + \mathcal{O}(\nu^5). \quad (3.92)$$

<sup>1</sup>This has led to many confusions in the conventional WKB literature and to some erroneous formulae in famous textbooks. In particular, the formula for the energy gap of the double-well potential in [34] is not correct. A discussion with a partial (but not fully accurate) fix can be found in [35].

The logarithmic term comes from the logarithmic singularity in (3.88), while the terms in  $1/\nu^{2k-1}$  come from  $\Pi_{\text{WKB}}^{(k)}(E)$  with  $k \geq 1$ . The correct prefactor in (3.89) can be obtained by promoting the series above, after exponentiation, to

$$\frac{\sqrt{2\pi}}{\Gamma\left(\nu + \frac{1}{2}\right)}. \quad (3.93)$$

This can be justified by an explicit all-orders calculation of the singular part of the period in the exact WKB method [36, 37], or by using the uniform WKB method [33] (see [2] for a pedagogical discussion.) Similarly, in the case of the cubic well, the imaginary part of the energy for an arbitrary level  $\nu$  is [38]

$$\text{Im } E(\nu) \approx -\frac{1}{4\pi} \frac{\partial E}{\partial \nu} e^{-\Pi_{\text{WKB}}(E; \hbar)/\hbar}. \quad (3.94)$$

It conventional quantum mechanics, and when  $\hbar \rightarrow 0$ , the exact WKB formulae above lead to the usual instanton results. The formulae (3.80) and (3.83) are identical to the standard ones, except that they involve the periods appropriate for deformed quantum mechanics. This suggests that the expressions (3.89) and (3.94) are also valid in the WKB approach to deformed quantum mechanics, provided we use the quantum periods adapted to the finite difference equation (2.4). This means in particular that the leading non-perturbative contribution is only due to the tunneling period.

Let us then briefly address the construction of formal quantum periods in deformed quantum mechanics. This problem was already considered in [17] and was revisited more recently in [19, 20]. In analogy with conventional quantum mechanics, one uses the difference equation (2.4) to define a quantum Liouville differential  $p(x; \hbar)dx$ , where  $p(x; \hbar)$  is given by a formal power series

$$p(x; \hbar) = \sum_{n \geq 0} p_n(x) \hbar^{2n}, \quad (3.95)$$

and

$$p_0(x) = \cosh^{-1}(Q(x)), \quad Q(x) = u(x) - 1 - E. \quad (3.96)$$

The higher order corrections can be computed systematically. For example,

$$p_1(x) = -\frac{1}{12} \frac{(Q^2(x) + 2)Q''(x)}{(Q^2(x) - 1)^{3/2}} + \frac{Q(x)(Q'(x))^2(13 + 2Q^2(x))}{24(Q^2(x) - 1)^{5/2}}. \quad (3.97)$$

Quantum periods are obtained by integration of this differential around the appropriate cycles. Tunneling periods are obtained by analytic continuation under the barriers, as in the usual WKB method. For example, the leading term of the tunneling period corresponding to (3.88) is

$$\Pi(E) = 2 \int_{x_0(E)}^{x_*^-(E)} \cos^{-1}(1 + E - u(z)) dz. \quad (3.98)$$

Since we will not consider quantum corrections in this section, we will suppress the superscript in  $\Pi$  that we used in (3.88).

Let us now compute the energy gap (3.89) and the imaginary part of the energy (3.94) by using the periods of deformed quantum mechanics, instead of the conventional ones, in the limit  $\hbar \rightarrow 0$  for fixed  $\nu$ . To do this we only need the classical period at order  $E$  and the analogue of

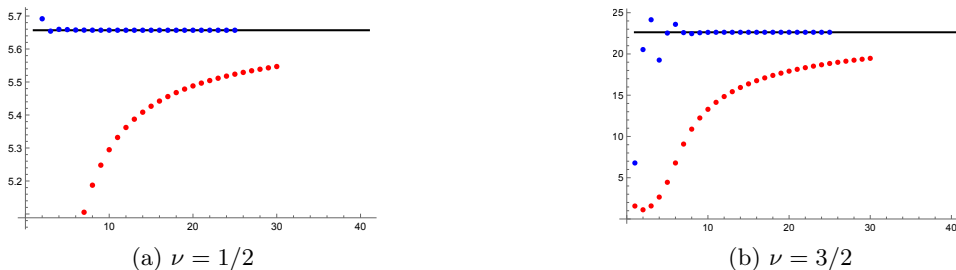


**Figure 6:** The energy difference  $\Delta E$  at the first ( $\nu = 1/2$ , left) and the second ( $\nu = 3/2$ , right) energy levels of the double-well model with  $h = 2$  and  $\hbar = 1/n$  ( $n = 1, 2, \dots$ ). The red dots are the numerical values of the energy differences divided by the exponential  $e^{-S/\hbar + 2\nu\mathcal{A}}$ . The blue dots are the results of Richardson transform to accelerate the numerical convergence. The black lines are the analytic values from the prefactors in (3.100).

the quantum corrections (3.92). These turn out to be the same in the case of deformed quantum periods, since (3.92) captures the local information near the minima of the potential. This can be explicitly checked by using e.g. (3.97). Since  $E$  is of order  $\hbar$ , we have to analyze the behavior of  $\Pi(E)$  when  $E = 0$ . As in the calculation of the period (3.69), this contains a logarithmic singularity in  $E$  due to the coalescence of the two points  $x_\star^\pm(E)$ . To extract this singularity, as well as the leading term in the regular part, it is better to take first a derivative w.r.t.  $E$ , and then use the tricks in (3.73) and (3.75). In this way one finds,

$$\Pi(E) = \mathcal{S} + \frac{E}{\omega} (\log(2E) - E) - \frac{2E}{\omega} (\mathcal{A} + \log(2\omega(x_\star - x_0))) + \dots, \quad (3.99)$$

where  $\mathcal{A}$  is given in (3.74). A simple calculation, after taking into account that  $\exp(-\nu(\log \nu - 1))$  has to be promoted to (3.93), gives

$$\Delta E(\nu) \approx -\frac{\hbar\omega}{\pi} \frac{\sqrt{2\pi}}{\Gamma(\nu + \frac{1}{2})} \left( \frac{2\omega(x_\star - x_0)^2}{\hbar} \right)^\nu e^{-S/\hbar + 2\nu\mathcal{A}} \quad (3.100)$$

for the  $\hbar \rightarrow 0$  asymptotics of the energy gap at the shifted level  $\nu$  in the double well. For the imaginary part of the energy in the cubic potential we find

$$\text{Im } E(\nu) \approx -\frac{\hbar\omega}{4\pi} \frac{\sqrt{2\pi}}{\Gamma(\nu + \frac{1}{2})} \left( \frac{2\omega(x_\star - x_0)^2}{\hbar} \right)^\nu e^{-S/\hbar + 2\nu\mathcal{A}}. \quad (3.101)$$

Both (3.100) and (3.101) can be checked against the numerical results by Hamiltonian matrix diagonalization, and they are found to give the correct results with high precision, as shown in Figs. 6 and Figs. 7 respectively.

## 4 Weak coupling phase and tunneling suppression

### 4.1 Complexifying the instantons

As we mentioned in the previous section, the standard instanton analysis is only valid when the parameter  $h$  in the potentials is smaller than a certain critical value. What happens when  $h > h_c$ ? We can simply try to analytically continue the quantities characterizing the instanton past this



**Figure 7:** Imaginary parts of the ground state energy ( $\nu = 1/2$ , left) and the first excited state energy ( $\nu = 3/2$ , right) of the cubic model with  $h = 1/2$  and  $\hbar = 1/(2n)$  ( $n = 1, 2, \dots$ ). The red dots are the numerical values of the imaginary parts divided by the exponential  $e^{-S/\hbar+2\nu\mathcal{A}}$ . The blue dots are the results of Richardson transform to accelerate the numerical convergence. The black lines are the analytic values from the prefactors in (3.101).

value. We first note that the potential crosses the value  $u(x) = 2$  at two points in the intermediate region of the potential. We denote them by  $x_{\text{np}}^{\pm}(E)$ , where np stands for “non-perturbative” (the reasons for this name is that these points characterize the new tunneling periods, as we will see). These points satisfy

$$u(x_{\text{np}}^{\pm}(E)) = 2. \quad (4.1)$$

In the double well they are given by

$$x_{\text{np}}^{\pm}(E) = \pm \sqrt{\frac{h}{2} - \sqrt{4 + E}}, \quad (4.2)$$

and in the cubic potential they satisfy

$$x_0(E) < x_{\text{np}}^{-}(E) < x_{\text{np}}^{+}(E) < x_{\star}(E) \quad (4.3)$$

(we recall that in this potential  $x_0(E)$  is the turning point for the energy  $E$ ). Like before, we will denote by  $x_{\text{np}}^{\pm} = x_{\text{np}}^{\pm}(0)$  the values at zero energy. The action (3.79) now becomes complex, since the integrand is complex in the interval  $[x_{\text{np}}^{-}, x_{\text{np}}^{+}]$ , and we find

$$\mathcal{S} = \mathcal{S}_{\mathbb{R}} + i\mathcal{S}_{\mathcal{I}}, \quad (4.4)$$

where

$$\mathcal{S}_{\mathbb{R}} = 2 \int_{x_{\text{np}}^{+}}^{x_{\star}} \cos^{-1}(1 - u(x)) dx + 2\pi x_{\text{np}}^{+}, \quad \mathcal{S}_{\mathcal{I}} = -2 \int_0^{x_{\text{np}}^{+}} \cosh^{-1}(u(x) - 1) dx, \quad (4.5)$$

for the double well, and

$$\begin{aligned} \mathcal{S}_{\mathbb{R}} &= 2 \left( \int_{x_0}^{x_{\text{np}}^{-}} + \int_{x_{\text{np}}^{+}}^{x_{\star}} \right) \cos^{-1}(1 - u(x)) dx + 2\pi (x_{\text{np}}^{+} - x_{\text{np}}^{-}), \\ \mathcal{S}_{\mathcal{I}} &= -2 \int_{x_{\text{np}}^{-}}^{x_{\text{np}}^{+}} \cosh^{-1}(u(x) - 1) dx, \end{aligned} \quad (4.6)$$

for the cubic potential. A similar complexification occurs for the quantity  $\mathcal{A}$  in (3.74) appearing in the one-loop correction to the instanton amplitude, and we will write it as

$$\mathcal{A} = \mathcal{A}_{\mathbb{R}} + i\mathcal{A}_{\mathcal{I}}. \quad (4.7)$$

We have

$$\mathcal{A}_{\mathbb{R}} = \int_{x_{\text{tp}}^+}^{x_{\star}} \frac{\omega dx}{\sqrt{u(x)(2-u(x))}} - \int_{x_0}^{x_{\star}} \frac{dx}{x_{\star} - x}, \quad \mathcal{A}_{\mathcal{I}} = \int_0^{x_{\text{np}}^+} \frac{\omega dx}{\sqrt{u(x)(u(x)-2)}}, \quad (4.8)$$

for the double well, and

$$\begin{aligned} \mathcal{A}_{\mathbb{R}} &= \left( \int_{x_0}^{x_{\text{np}}^-} + \int_{x_{\text{np}}^+}^{x_{\star}} \right) \frac{\omega dx}{\sqrt{u(x)(2-u(x))}} - \int_{x_0}^{x_{\star}} \frac{dx}{x_{\star} - x}, \\ \mathcal{A}_{\mathcal{I}} &= \int_{x_{\text{np}}^-}^{x_{\text{np}}^+} \frac{\omega dx}{\sqrt{u(x)(u(x)-2)}}, \end{aligned} \quad (4.9)$$

for the cubic well<sup>2</sup>.

Since the instantons have become complex, they have an imaginary phase which might lead to tunneling suppression, as it happens e.g. in the spin systems studied in [7, 8]. We note that in conventional quantum mechanics, and for the potentials we are considering, complex instantons do not occur for the low energy levels, and tunneling is never suppressed<sup>3</sup>. The existence of complex instantons in deformed quantum mechanics is ultimately due to the unconventional kinetic term in the Hamiltonian. The complexification of the instantons can be also seen in the Euclidean EOM (3.22) and Figs. 1b, 2b, involving the effective inverted potential  $w(x; E)$ : as  $\hbar$  grows to its critical value, the bump in the middle of the well for  $w(x; E)$  grows up and “cuts” the instanton trajectory.

Let us now see how we can incorporate these complex instantons in the calculation of the non-perturbative effects. One obvious approach is to add up the contribution of the complex instanton and its complex conjugate. This is the procedure suggested in the seminal paper [40] and reviewed in section 3.5 of [3]. When applied to the double-well potential, we find the result

$$\Delta E(\nu) \approx -\frac{2\hbar\omega}{\pi} \frac{\sqrt{2\pi}}{\Gamma(\nu + \frac{1}{2})} \left( \frac{2\omega(x_{\star} - x_0)^2}{\hbar} \right)^{\nu} \cos \left( \frac{\mathcal{S}_{\mathcal{I}}}{\hbar} - 2\nu\mathcal{A}_{\mathcal{I}} \right) e^{-\mathcal{S}_{\mathbb{R}}/\hbar + 2\nu\mathcal{A}_{\mathbb{R}}}. \quad (4.10)$$

This formula leads indeed to tunneling suppression, due to the cos term. We note that, although we have not indicated it explicitly, the energy gap is given, strictly speaking, by the absolute value of the above expression, since when tunneling suppression happens, the roles of the ground state and the first excited state are interchanged. We will verify in a moment that this is indeed the instanton approximation to the exact formula conjectured in [10]. In addition, a direct calculation of the spectrum of the Hamiltonian for  $\hbar > \hbar_c$  shows that this formula describes the correct asymptotic behaviour of the energy gap at small  $\hbar$ . Let us evaluate numerically the function

$$\Delta \mathcal{E}(\nu, \hbar) := |(2/\hbar)^{1-\nu} (\pi/2)^{1/2} \Gamma(\nu + 1/2) e^{\mathcal{S}_{\mathbb{R}}/\hbar - 2\nu\mathcal{A}_{\mathbb{R}}} \Delta E(\nu, \hbar)| \quad (4.11)$$

<sup>2</sup>The sign of  $\mathcal{A}_{\mathcal{I}}$  involves a choice of sign in the square root in (4.8). This can be fixed by noting that  $\mathcal{A}_{\mathcal{I}}$  is the subleading term in the expansion of the energy-dependent WKB period around  $E = 0$ .

<sup>3</sup>Complex instantons appear and play a rôle in the double-well for energies above the barrier, see e.g. section 5.2 of [39], but this is a very different situation from what we have here, since classical motion between the critical points is no longer forbidden in that case.

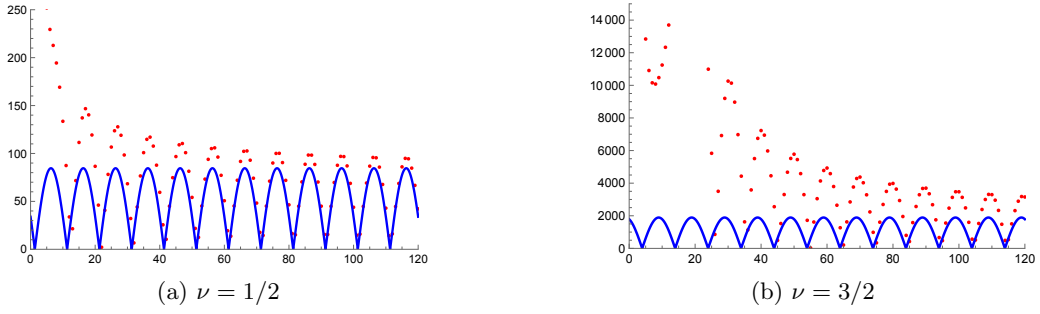


**Figure 8:** The function  $\Delta\mathcal{E}(\nu, \hbar)$  evaluated on the sequence  $\hbar_n^{(1)}$  for (a)  $\nu = 1/2$  and (b)  $\nu = 3/2$  with  $h = 10$ . The red dots are numerical results, and the blue curve is the prediction from complexification of instantons.

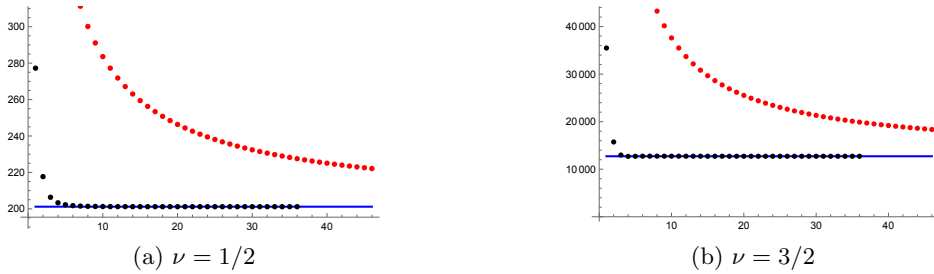


**Figure 9:** The function  $\Delta\mathcal{E}(\nu, \hbar)$  evaluated on the sequence  $\hbar_n^{(2)}$  for (a)  $\nu = 1/2$  and (b)  $\nu = 3/2$  with  $h = 20$ . The red dots are numerical results, the black dots are results after applying the Richardson transform to speed up the convergence, and the blue line is the asymptotic value predicted from complexification of instantons.

on a sequence of  $\hbar$ ,

$$\hbar_n^{(1)} = -10\mathcal{S}_{\mathcal{I}}/(\pi n), \quad n = 1, 2, 3, \dots \quad (4.12)$$

Eq. (4.10) predicts that in the large  $n$  limit the value of  $\Delta\mathcal{E}(\nu, \hbar_n^{(1)})$  should oscillate following the pattern

$$\Delta\mathcal{E}(\nu, \hbar_n^{(1)}) \approx 4\omega^{1+\nu}(x_* - x_0)^{2\nu} |\cos(-(\pi/10)n - 2\nu\mathcal{A}_{\mathcal{I}})|. \quad (4.13)$$

As illustrated in Figs. 8, we find that this is indeed the case for both  $\nu = 1/2$  and  $\nu = 3/2$ . The numerical value of  $\Delta\mathcal{E}(\nu, \hbar_n^{(1)})$  and the right hand side of (4.13) oscillate locked in phase and they reach crests and troughs at the same time. In addition, the amplitude of oscillation of  $\Delta\mathcal{E}(\nu, \hbar_n^{(1)})$  seems to asymptote to that of the right hand side of (4.13) in the large  $n$  limit. To make a higher precision check of the latter statement, we evaluate  $\Delta\mathcal{E}(\nu, \hbar)$  on a second sequence of  $\hbar$

$$\hbar_n^{(2)} = -\mathcal{S}_{\mathcal{I}}/(\pi n + \mathcal{A}_{\mathcal{I}}), \quad n = 1, 2, 3, \dots \quad (4.14)$$

According to (4.10) its value should asymptote to the maximum value of the right hand side of (4.13),

$$\Delta\mathcal{E}(\nu, \hbar_n^{(2)}) \approx 4\omega^{1+\nu}(x_* - x_0)^{2\nu}, \quad (4.15)$$

which is indeed verified, as shown in Figs. 9.

However, if we apply the same procedure to the cubic potential, and we simply take into account the contribution of the complex instanton and its conjugate, the resulting formula for the imaginary part of the energy turns out to be incorrect. This means that the structure of the instantons of the theory is more complicated. In particular, naif complexification fails. We will now explain why this is so and why the naif approach is not guaranteed to be valid in general.

## 4.2 Resurgent analysis and Stokes constants

Determining the correct instanton content in a quantum mechanical model can be challenging. The conventional picture of instantons as classical solutions of the Euclidean EOM, which we used successfully in section 3, does not always give a reliable guide, in particular in situations where complex instantons arise. We have just seen that the naif complexification of the instantons in the cubic potential seems to miss crucial information. One needs a more general setting which, in conventional one-dimensional quantum mechanics, was put forward in the seminar work of Voros and collaborators, also called the exact complex WKB method [41, 42]. The first lesson of this method is that, in order to obtain the collection of possible non-perturbative corrections or trans-series, one should consider a lattice of instanton actions in the complex plane (or more generally, a lattice of complex periods of the underlying classical Hamiltonian, regarded as an algebraic curve). To each point  $\mathcal{S}$  of this lattice one can associate trans-series weighted by the exponentially small term  $\exp(-\mathcal{S}/\hbar)$ . In order to determine which are the instantons in this lattice that contribute to a given quantity, one has to perform a detailed analysis which involves the Voros–Silverstone connection formula for the Schrödinger operator [42, 43] (see [2] for a pedagogical exposition).

In the context of difference equations, the precise analogue of the Voros–Silverstone connection formula is not known, although it is expected to be more complicated. To have a handle on our problem we will use a shortcut and appeal to the theory of resurgence. According to this theory, some of the non-perturbative corrections which are needed in a problem (but not necessarily all) can be read from the large order behaviour of perturbation theory (see [3] for a readable introduction to the subject). This method can fail in special situations, mostly due to the presence of symmetries. For example, in the double-well potential in conventional quantum mechanics, the large order behavior of the perturbative series misses the one-instanton correction to the energy gap (as we will see, this is also the case in the deformed double-well). However, in the case of the cubic well potential, the instanton effect responsible for the imaginary part of the energy is completely captured by the large order behavior of the perturbative series, or equivalently, by the structure of Borel singularities of its Borel transform. We will then analyze the resurgent structure of the perturbative series in deformed quantum mechanics to extract the missing information on the instanton contributions.

We first give a lightning review of the basic ideas in the theory of resurgence, mostly to fix the notation. Let us consider a formal series

$$\phi(z) = \sum_{n=0}^{\infty} a_n z^n, \quad a_n \approx n!, \quad (4.16)$$

whose coefficients grow factorially. Its Borel transform

$$\widehat{\phi}(\zeta) = \sum_{n=0}^{\infty} \frac{a_n}{n!} \zeta^n, \quad (4.17)$$

has a finite radius of convergence and in favourable circumstances can be analytically continued to the complex planes, where it will have singularities. We also assume that  $\widehat{\phi}(\zeta) \lesssim \exp(|\zeta|/R)$

i.e. it grows at most exponentially fast with  $z < R$ . The Borel resummation of the original series  $\phi(z)$  is then given by

$$\mathcal{S}\phi(z) = \frac{1}{z} \int_0^\infty \widehat{\phi}(\zeta) e^{-\zeta/z} d\zeta, \quad (4.18)$$

The existence of the Borel resummation depends crucially on the distribution of the singular points of  $\widehat{\phi}(\zeta)$  in the complex  $\zeta$ -plane, called the Borel plane. If  $\widehat{\phi}(\zeta)$  has singularities on the positive real axis, (4.18) is ill-defined and the original series  $\phi(z)$  is said to be not Borel summable. Instead, one defines a pair of lateral Borel resummations,

$$\mathcal{S}^{(\pm)}\phi(z) = \frac{1}{z} \int_0^{e^{\pm i0^+}\infty} \widehat{\phi}(\zeta) e^{-\zeta/z} d\zeta. \quad (4.19)$$

This definition can be generalized to

$$\mathcal{S}^{(\theta)}\phi(z) = \frac{1}{z} \int_0^{e^{i\theta}\infty} \widehat{\phi}(\zeta) e^{-\zeta/z} d\zeta. \quad (4.20)$$

for  $|\theta| < \pi/2$ , and it coincides with the positive (negative) lateral resummation when  $\theta > 0$  (resp.  $\theta < 0$ ) if the Borel transform  $\widehat{\phi}(\zeta)$  has no additional singularities between the positive real axis  $\mathbb{R}_+$  and the ray  $\rho_\theta = e^{i\theta}\mathbb{R}_+$  in the Borel plane. Due to the singular points on the positive real axis, the two lateral resummations differ by a non-perturbatively small quantity, and their difference, known as the Stokes discontinuity<sup>4</sup>

$$\text{disc}_0\phi(z) = \mathcal{S}^{(+)}\phi(z) - \mathcal{S}^{(-)}\phi(z), \quad (4.21)$$

is controlled by these singular points. Let the singularities be located at  $\mathcal{S}_1 < \mathcal{S}_2 < \dots$ , and let us suppose that each of them is associated with an additional power series

$$\varphi^{(i)}(z) = \sum_{n=0}^{\infty} a_n^{(i)} z^n. \quad (4.22)$$

Then, the Stokes discontinuity is given by

$$\text{disc}_0\phi(z) = \sum_{i \geq 1} S_i \mathcal{S}^{(-)}\varphi^{(i)}(z), \quad \varphi^{(i)}(z) = z^{-\nu_i} e^{-S_i/z} \varphi^{(i)}(z), \quad (4.23)$$

where the Borel resummation on the right hand is applied on the power series  $\varphi^{(i)}(z)$ . The coefficients  $S_i$  are known as Stokes constants, and their value depends on a choice of normalization for  $\varphi^{(i)}$ . Clearly, the distribution of singular points of  $\widehat{\phi}(\zeta)$ , the power series associated to them, as well as the Stokes constants, are crucial for making sense of the asymptotic series  $\phi(z)$  via Borel resummation, and they are known collectively as the resurgence structure of  $\phi(z)$ .

Let us now explore the resurgent structure of our models. We first look at the cubic model with Hamiltonian  $H_3$  (2.7). Let us consider the perturbative series for the energy  $E^{\text{pert}}(\nu, \hbar)$  at fixed shifted level  $\nu$ . This series can be efficiently calculated to hundreds of terms by using the `Mathematica` package `BenderWu` [44, 45]. We find

$$E^{\text{pert}}(\nu, \hbar) = (3\hbar)^{1/4} \nu \hbar + \left( \left( -\frac{7}{192\hbar} + \frac{\sqrt{3\hbar}}{64} \right) + \left( -\frac{5}{16\hbar} + \frac{\sqrt{3\hbar}}{16} \right) \nu^2 \right) \hbar^2 + \mathcal{O}(\hbar^3). \quad (4.24)$$

---

<sup>4</sup>The subscript 0 refers to the branch of zero inclination angle across which the discontinuity is calculated.

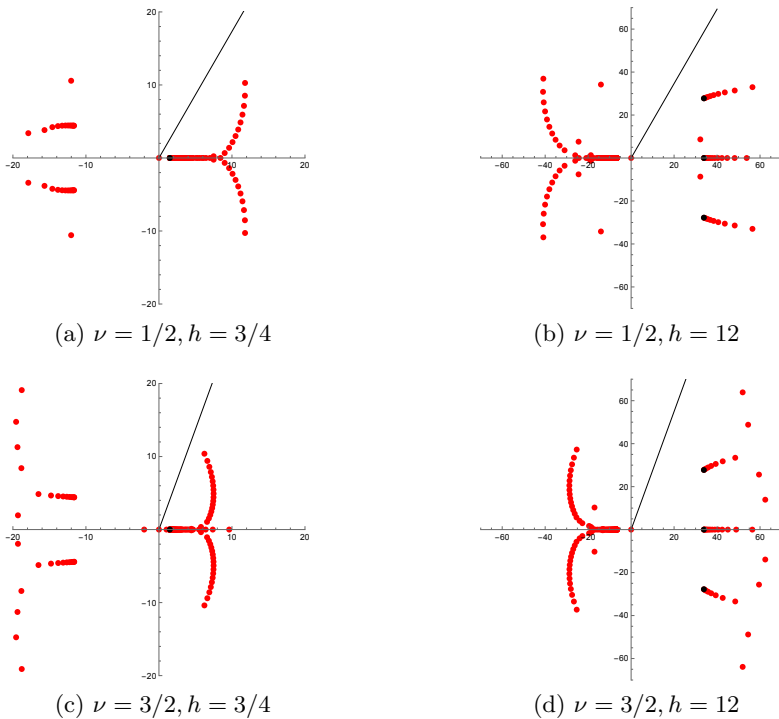


**Figure 10:** The Borel plane of the perturbative energy series of the cubic model at both  $\nu = 1/2$  (upper) and  $\nu = 3/2$  (lower) for both  $h < h_c$  (left) and  $h > h_c$  (right). The red dots are position of poles of Padé approximant of the Borel transform of the perturbative series truncated up to 300 terms. The black dots are the position of the branch points. The black lines are the integration contour for the (upper) lateral Borel resummation, which are raised at  $60^\circ$  for  $\nu = 1/2$  and at  $70^\circ$  for  $\nu = 3/2$ .

We first look at the case with  $h < h_c$ . The Borel planes for  $E^{\text{pert}}(\nu, \hbar)$  at  $\nu = 1/2$  and  $\nu = 3/2$  are shown in Figs. 10a, 10c. Singular points are found on the positive real axis, so that the perturbative series  $E^{\text{pert}}(\nu, \hbar)$  is not Borel summable. On the other hand, as demonstrated in Tab. 1, we find that the lateral Borel resummation  $\mathcal{S}^{(+)}E^{\text{pert}}(\nu, \hbar)$  agrees with the numerical evaluation of the energy  $E(\nu, \hbar)$  obtained by Hamiltonian matrix diagonalization:

$$\mathcal{S}^{(+)}E^{\text{pert}}(\nu, \hbar) = \mathcal{S}^{(\theta_+)}E^{\text{pert}}(\nu, \hbar) = E(\nu, \hbar), \quad h < h_c. \quad (4.25)$$

This is similar to what happens in the cubic well in conventional quantum mechanics. Note that in the evaluation of  $\mathcal{S}^{(+)}E^{\text{pert}}(\nu, \hbar)$  we need to significantly raise the inclination angle  $\theta_+$  of the integration contour in order to avoid all the singular points that trail off from those on the positive real axis<sup>5</sup>, and this is emphasized by the notation  $\mathcal{S}^{(\theta_+)}E^{\text{pert}}(\nu, \hbar)$  in the middle of the identity above. From the definition of lateral resummation (4.19), we also have

$$\mathcal{S}^{(-)}E^{\text{pert}}(\nu, \hbar) = \overline{E}(\nu, \hbar), \quad h < h_c, \quad (4.26)$$

<sup>5</sup>Note that moving to the right in the Borel plane the trail of singular points splits to two uncanny branches, which stem from our limited precision in calculating the Borel transform  $\tilde{E}^{\text{pert}}(\nu, \zeta)$  by using a truncated perturbative series and Padé approximant as means for analytic continuation.

$\nu = 1/2$	$\hbar = 1$	$\hbar = 1/3$
$\mathcal{S}^{(+)} E^{\text{pert}}(\hbar)$	0.53409747428 - i0.19689238266	0.18177567215412 - i0.00914131410440
$E^{\text{num}}(\hbar)$	0.53409747425 - i0.19689238261	0.18177567215419 - i0.00914131410448
$E^{(1)}(\hbar)$	$\mathcal{O}(0.1)$	$\mathcal{O}(0.01)$
$\nu = 3/2$	$\hbar = 1$	$\hbar = 1/3$
$\mathcal{S}^{(+)} E^{\text{pert}}(\hbar)$	1.804970 - i1.168308	0.505013430505 - i0.137929992127
$E^{\text{num}}(\hbar)$	1.804960 - i1.168316	0.505013430512 - i0.137929992119
$E^{(1)}(\hbar)$	$\mathcal{O}(1)$	$\mathcal{O}(0.1)$

**Table 1:** Comparison of the (upper) lateral Borel resummed perturbative energy series  $\mathcal{S}^{(+)} E^{\text{pert}}(\nu, \hbar)$  and the numerical evaluation of the eigen-energy  $E^{\text{num}}(\nu, \hbar)$  at  $\nu = 1/2$  and  $\nu = 3/2$  for  $h = 3/4$ . The lateral resummation is performed with perturbative series truncated to 300 terms and with integration contour inclined at  $60^\circ$  ( $\nu = 1/2$ ) and  $70^\circ$  ( $\nu = 3/2$ ). The numerical evaluation is performed by diagonalizing the Hamiltonian matrix using the eigenstates of harmonic oscillator with  $\omega = 1$  as basis vectors truncated to rank 100. For reference, the estimates of 1-instanton correction  $E^{(1)}(\hbar)$  calculated by (4.32) are also given.

so that

$$\text{Im } E(\nu, \hbar) = \frac{1}{2i} \text{disc}_0 E^{\text{pert}}(\nu, \hbar) = \frac{1}{2i} \mathcal{S}^{(-)} E^{(1)}(\nu, \hbar) + \dots, \quad h < h_c, \quad (4.27)$$

and we have chosen a normalization so that  $S_1 = 1$  for the leading singular point. In the small  $\hbar$  limit, the imaginary part of the ground state energy is related to the non-perturbative corrections by

$$\text{Im } E(\nu, \hbar) \approx \frac{1}{2i} E^{(1)}(\nu, \hbar), \quad h < h_c. \quad (4.28)$$

By numerical evaluation, we find indeed that

$$E^{(1)}(\nu, \hbar) \approx -\frac{i\hbar\omega}{\sqrt{2\pi}\Gamma(\nu + \frac{1}{2})} \left( \frac{2\omega(x_* - x_0)^2}{\hbar} \right)^\nu e^{-S/h + 2\nu\mathcal{A}}, \quad h < h_c, \quad (4.29)$$

in agreement with (3.101), which is reassuring. Note that the right hand side of the formula above has the same form as  $\phi^{(i)}$  in (4.23), and the instanton action  $\mathcal{S}$  agrees with the location of the leading singular point in Fig. 10a, indicating that the latter plays the role of the branch point at the head of a branch cut. Furthermore, there are also singular points on the left half of the Borel plane, but they are irrelevant from the definition of the lateral resummations (4.19) and (4.20) as long as we are only concerned with the Borel resummation of the perturbative energy with  $\hbar > 0$ .

Next, we switch to the case when  $h > h_c$ . The Borel plane is given in Fig. 10b. In contrast to the previous case, the single singular point on the positive real axis splits to *three singular points*, where the additional two are above and below the positive real axis. It turns out that the suitable way to define the (upper) lateral Borel resummation is to raise the inclination  $\theta_+$  of the integration contour high enough so that it goes over all the three branch cuts, as indicated in Fig. 10b. Then we find numerically

$$\mathcal{S}^{(+)} E^{\text{pert}}(\nu, \hbar) := \mathcal{S}^{(\theta_+)} E^{\text{pert}}(\nu, \hbar) = E(\nu, \hbar), \quad h > h_c, \quad (4.30)$$

as demonstrated in Tab. 2.

This is actually quite natural from the resurgence point of view. We can fix the inclination angle  $\theta_+$  of the integral contour for the (upper) lateral resummation so that the contour is both above the branch cut along the positive real axis (as well as the spurious poles) when  $h < h_c$  and over all the three branch cuts when  $h > h_c$ , as in Fig. 10. When we change continuously the value of  $h$  from smaller than  $h_c$  to greater than  $h_c$ , no singular points of the Borel transform  $\widehat{E}^{\text{pert}}(\nu, \zeta)$  cross the integral contour in the Borel plane, and consequently the value of the (upper) lateral resummation  $\mathcal{S}^{(\theta_+)} E^{\text{pert}}(\nu, \hbar)$  changes continuously. As the exact value of  $E(\nu, \hbar)$  also changes continuously in the process, these two functions should agree both when  $h < h_c$  and when  $h > h_c$ .

Using the same trick as (4.26), we then conclude that

$$\begin{aligned} \text{Im } E(\nu, \hbar) &= \mathcal{S}^{(+)} E^{\text{pert}}(\nu, \hbar) - \mathcal{S}^{(-)} E^{\text{pert}}(\nu, \hbar) \\ &\approx \frac{1}{2i} \left( \mathbf{S}_1 E^{(1)}(\nu, \hbar) + \mathbf{S}_{1+} E^{(1+)}(\nu, \hbar) + \mathbf{S}_{1-} E^{(1-)}(\nu, \hbar) \right) + \dots, \quad h > h_c, \end{aligned} \quad (4.31)$$

where  $E^{(1)}(\nu, \hbar)$ ,  $E^{(1+)}(\nu, \hbar)$ ,  $E^{(1-)}(\nu, \hbar)$  are associated to the singularities on, above, and below the positive real axis respectively. By evaluating numerically the Stokes discontinuities across these three individual branch cuts, we find that

$$E^{(1)}(\nu, \hbar) = -\frac{i\hbar\omega}{\sqrt{2\pi}\Gamma(\nu + \frac{1}{2})} \left( \frac{2\omega(x_\star - x_0)^2}{\hbar} \right)^\nu e^{-\mathcal{S}_{\mathbb{R}}/\hbar + 2\nu\mathcal{A}_{\mathbb{R}}}, \quad (4.32a)$$

$$E^{(1\pm)}(\nu, \hbar) = -\frac{i\hbar\omega}{\sqrt{2\pi}\Gamma(\nu + \frac{1}{2})} \left( \frac{2\omega(x_\star - x_0)^2}{\hbar} \right)^\nu e^{-(\mathcal{S}_{\mathbb{R}} \pm i\mathcal{S}_{\mathcal{I}})/\hbar + 2\nu(\mathcal{A}_{\mathbb{R}} \pm i\mathcal{A}_{\mathcal{I}})}, \quad (4.32b)$$

and the associated Stokes constants are

$$\mathbf{S}_1 = 2, \quad \mathbf{S}_{1\pm} = 1. \quad (4.33)$$

Consequently, we should have

$$\text{Im } E(\nu, \hbar) \approx -\frac{\hbar\omega}{\sqrt{2\pi}\Gamma(\nu + \frac{1}{2})} \left( \frac{2\omega(x_\star - x_0)^2}{\hbar} \right)^\nu \left( 1 + \cos\left(\frac{\mathcal{S}_{\mathcal{I}}}{\hbar} - 2\nu\mathcal{A}_{\mathcal{I}}\right) \right) e^{-\mathcal{S}_{\mathbb{R}}/\hbar + 2\nu\mathcal{A}_{\mathbb{R}}}. \quad (4.34)$$

The formula (4.34) can also be tested directly by the method discussed at the end of section 4.1. Let us evaluate numerically the function

$$\text{Im } \mathcal{E}(\nu, \hbar) := -(2/\hbar)^{1-\nu} (\pi/2)^{1/2} \Gamma(\nu + 1/2) e^{\mathcal{S}_{\mathbb{R}}/\hbar - 2\nu\mathcal{A}_{\mathbb{R}}} \text{Im } E(\nu, \hbar) \quad (4.35)$$

on a sequence of  $\hbar$ ,

$$\hbar_n^{(1)} = -10\mathcal{S}_{\mathcal{I}}/(\pi n), \quad n = 1, 2, 3, \dots \quad (4.36)$$

Eq. (4.34) predicts that the value of  $\text{Im } \mathcal{E}(\nu, \hbar_n^{(1)})$  should oscillate following the pattern

$$\text{Im } \mathcal{E}(\nu, \hbar_n^{(1)}) \approx \omega^{1+\nu} (x_\star - x_0)^{2\nu} (1 + \cos(-(\pi/10)n - 2\nu\mathcal{A}_{\mathcal{I}})), \quad (4.37)$$

in the large  $n$  limit. As illustrated by Fig. 11, we find that this is indeed the case for both  $\nu = 1/2$  and  $\nu = 3/2$ : not only do the value of  $\text{Im } E(\nu, \hbar_n^{(1)})$  and the prediction from the resurgence analysis (4.37) oscillate locked in phase, the amplitude of oscillation of  $\text{Im } \mathcal{E}(\nu, \hbar_n^{(1)})$  also asymptotes to that of (4.37) in the large  $n$  limit. To test with higher numerical precision the

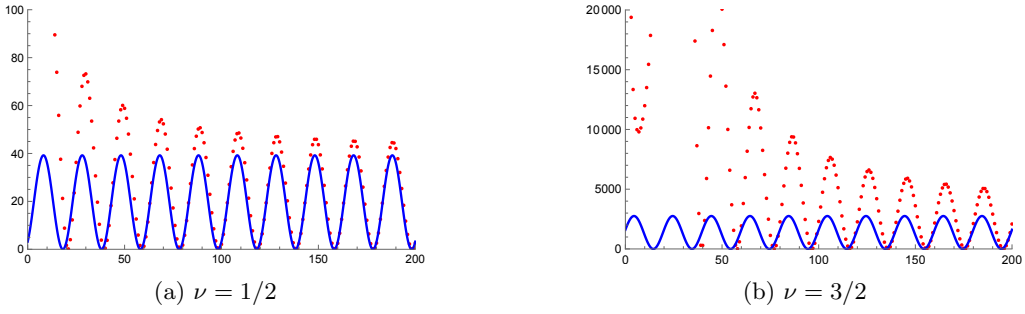


**Figure 11:** The function  $\text{Im } \mathcal{E}(\nu, \hbar)$  evaluated on the sequence  $\hbar_n^{(1)}$  for (a)  $\nu = 1/2$  and (b)  $\nu = 3/2$  with  $h = 10$ . The red dots are numerical results, and the blue curve is the prediction from resurgency analysis.

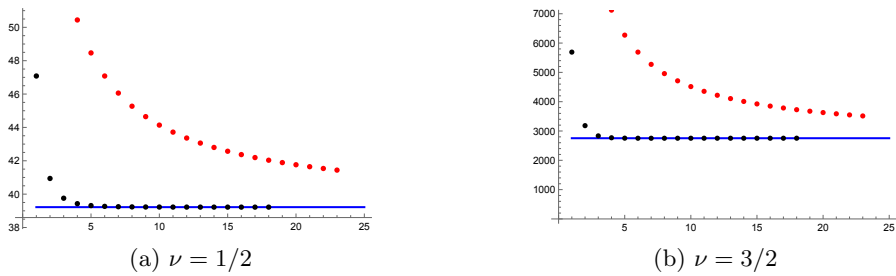


**Figure 12:** The function  $\text{Im } \mathcal{E}(\nu, \hbar)$  evaluated on the sequence  $\hbar_n^{(2)}$  for (a)  $\nu = 1/2$  and (b)  $\nu = 3/2$  with  $h = 10$ . The red dots are numerical results, the black dots are results after applying the Richardson transform to speed up the convergence, and the blue line is the asymptotic value predicted from resurgency analysis.

latter statement, as the prefactor in (4.37) is crucial, we evaluate  $\text{Im } \mathcal{E}(\nu, \hbar)$  on a second sequence of  $\hbar$

$$\hbar_n^{(2)} = -\mathcal{S}_{\mathcal{I}}/(2\pi n - \mathcal{A}_{\mathcal{I}}), \quad n = 1, 2, 3, \dots, \quad (4.38)$$

always at the crests of the oscillation, and its value should asymptote to the maximum value

$$\text{Im } \mathcal{E}(\nu, \hbar_n^{(2)}) \approx \omega^{1+\nu} (x_{\star} - x_0)^{2\nu}, \quad (4.39)$$

which is indeed verified as shown in Fig. 12.

The formula (4.34) shows that indeed the complexification of the instantons lead to tunneling suppression, as in the double well. However, the precise pattern for the vanishing of the imaginary part of the energy is due to the instanton with complex action, its conjugate, and an additional instanton with real action. The latter does not appear if we just use the naive complexification approach of [40]. It is also not obvious how to understand this real instanton in terms of complexified solutions to the EOM. In this case, however, the resurgent approach gives us a precise understanding of the non-perturbative corrections that have to be taken into account.

There is yet another perspective to understand the change of singularity structure in the Borel plane, and therefore the phase transition in the quantum mechanical model. The spectrum of BPS states of  $\mathcal{N} = 2$  super Yang–Mills theory is known to undergo wall-crossing at special loci in moduli space [12, 46], and the monopole points typically belong to this loci. It was shown

$\nu = 1/2$	$\hbar = 3/2$	$\hbar = 1$
$\mathcal{S}^{(+)} E^{\text{pert}}(\hbar)$	$2.158989556195731030 - i 2.48522 \times 10^{-13}$	$1.377257148742246102603174 - i 3.7969395719 \times 10^{-14}$
$E^{\text{num}}(\hbar)$	$2.158989556195731029 - i 2.48572 \times 10^{-13}$	$1.377257148742246102603189 - i 3.7969395749 \times 10^{-14}$
$E^{(1)}(\hbar)$	$\mathcal{O}(10^{-10})$	$\mathcal{O}(10^{-15})$
$\nu = 3/2$	$\hbar = 3/2$	$\hbar = 1$
$\mathcal{S}^{(+)} E^{\text{pert}}(\hbar)$	$6.8228767656714 - i 3.23338 \times 10^{-8}$	$4.33475553996766479544 - i 5.12436612 \times 10^{-12}$
$E^{\text{num}}(\hbar)$	$6.8228767656751 - i 3.23348 \times 10^{-8}$	$4.33475553996766479532 - i 5.12436607 \times 10^{-12}$
$E^{(1)}(\hbar)$	$\mathcal{O}(10^{-9})$	$\mathcal{O}(10^{-14})$

**Table 2:** Comparison of the (upper) lateral Borel resummed perturbative energy series  $\mathcal{S}^{(+)} E^{\text{pert}}(\nu, \hbar)$  and the numerical evaluation of the eigen-energy  $E^{\text{num}}(\nu, \hbar)$  at both  $\nu = 1/2$  and  $\nu = 3/2$  for  $h = 12$ . The convention is the same as in Tab. 1, except that for Borel resummation, the perturbative series is truncated to 400 terms for  $\nu = 3/2$ , and for numerical evaluation the Hamiltonian matrix is truncated to rank 250.

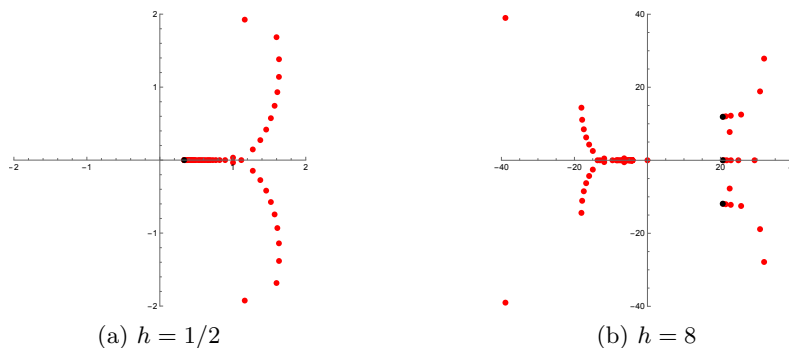


**Figure 13:** The Borel plane of the perturbative energy series of the double-well model at  $\nu = 1/2$  for both  $h < h_c$  (left) and  $h > h_c$  (right). The red dots are position of poles of Padé approximant of the Borel transform of the perturbative series truncated up to 150 terms. The black dots are the position of the branch points, which are located at  $2\mathcal{S}$  in the left plot, and at  $2\mathcal{S}_{\mathbb{R}}, 2\mathcal{S}_{\mathbb{R}} \pm 2i\mathcal{S}_{\mathcal{I}}$  in the right plot.

in [47] that this spectrum governs the singularity structure of the quantum periods associated to the quantum SW curve. Therefore, the phase structure in deformed quantum mechanics must be due ultimately to the wall-crossing in the  $\mathcal{N} = 2$ ,  $SU(3)$  Yang–Mills spectrum. The splitting of singularities we observe seems to be closely related to the appearance of a tower of particles in the weakly coupled phase of the  $\mathcal{N} = 2$  theory, as it happens in the  $SU(2)$  case. It would be interesting to make this more explicit.

We finally comment on the double-well model. The resurgence analysis can also be performed on the perturbative energy series for this model, which is calculated to be

$$E^{\text{pert}}(\nu, \hbar) = \sqrt{2\hbar\nu\hbar} + \left( \left( -\frac{1}{8h} + \frac{h}{32} \right) + \left( -\frac{3}{2h} + \frac{h}{8} \right) \nu^2 \right) \hbar^2 + \mathcal{O}(\hbar^3). \quad (4.40)$$

However, as shown in Figs. 13, the leading singularities of the Borel transform of the perturbative energy on the right half of the Borel plane are located at  $2\mathcal{S}$  or  $2\mathcal{S}_{\mathbb{R}}$  instead of at  $\mathcal{S}$ , indicating that it completely misses the one-instanton corrections to the energy, just like in the ordinary quantum mechanical model with a double-well potential (see e.g. [48] for a discussion.)

### 4.3 Comparison to the exact quantization conditions

One of the original reasons to consider the deformation of quantum mechanics studied in this paper was to have a testing ground and a simpler example of the TS/ST duality of [13, 14], which provides an explicit, exact solution of certain spectral problems in the quantum mechanics of Weyl operators via topological string theory. The Hamiltonian of deformed quantum mechanics turns out to be a special limit of the Weyl-like Hamiltonians considered in [13, 14].

The EQCs in [10] are expressed in terms of a special resummation of the quantum periods on the spectral curve

$$2\Lambda^N \cosh(p) + W_N(x) = 0, \quad (4.41)$$

where  $W_N(x)$  was defined in (2.5), and the Liouville form is  $p(x)dx$ . As mentioned in section 2, these periods can be obtained by using the so-called NS limit [25] of the instanton partition function [26, 27] of the underlying  $\mathcal{N} = 2$  super Yang–Mills theory. The details are not important for our purposes, since we will only need the classical limit of these periods. A more detailed description of the full quantum story can be found in [10]. There are two types of quantum periods in this game, the so-called  $A$  and  $B$  periods, which correspond to a choice of  $A$  and  $B$  cycles in the curve (4.41). We will denote them respectively by

$$a_i(\{h\}; \hbar), \quad \phi_i(\{h\}; \hbar), \quad i = 1, \dots, N. \quad (4.42)$$

The classical limit of the  $\phi_i(\{h\}; \hbar)$  as  $\hbar \rightarrow 0$ , which we will denote as  $\phi_i^{(0)}(\{h\}; \hbar)$ , are the classical periods which appear in the EBK quantization conditions of the Toda lattice (see e.g. [49] or section 2.12 of [2]). The EQCs of [10] are given by a single functional constraint on the quantum periods. One important remark is that the quantum periods appearing in the EQC are defined by Yang–Mills instanton partition sums, which do not converge everywhere in moduli space, and this might lead to limits in the applicability of these conditions, as already noted in [10]. Most relevant to our problem, when  $\hbar = 0$ , the instanton sums only converge in the weak coupling region, and for  $\hbar$  small we do not expect them to converge deep inside the strong coupling region. Therefore, in order to obtain the asymptotics of the non-perturbative effects in the strong coupling phase,  $h < h_c$ ,  $E = \mathcal{O}(\hbar)$ , and  $\hbar \rightarrow 0$ , one would have to make an extrapolation of the quantum periods beyond its region of convergence, a problem we will not address here.

Let us now write down the EQCs found in [10]. In the case of the double-well, symmetry reasons impose the following relationship between the periods:  $a_1 = a_3$ ,  $\phi_3 = \phi_2$ . The quantization conditions read

$$\cos\left(\frac{\phi_2}{2\hbar}\right) = \epsilon \mathcal{V} \sin\left(\frac{\phi_1 + \phi_2}{2\hbar}\right), \quad \epsilon = \pm(-1)^k, \quad (4.43)$$

where the sign  $\pm(-1)^k$  corresponds to the energy level  $E_{2k}$ ,  $E_{2k+1}$ , respectively, and  $\mathcal{V}$  is given by

$$\mathcal{V} = e^{-\pi a_2/\hbar} \frac{1 - e^{-2\pi a_1/\hbar}}{1 - e^{-2\pi(a_1+a_2)/\hbar}}. \quad (4.44)$$

We note that, in order to have an easier match with the conventions in this paper, we have redefined  $\phi_i \rightarrow \phi_i/\hbar$ , and changed the sign of  $\phi_2$  in the equations of [10].

To understand the EQC in detail, we have to be more precise about the quantum periods appearing in it. Let us first define the points  $x_\star^\pm(E)$  as the positive turning points of  $u(x)$  for an energy  $E$ :

$$u(x_\star^\pm(E)) = E. \quad (4.45)$$

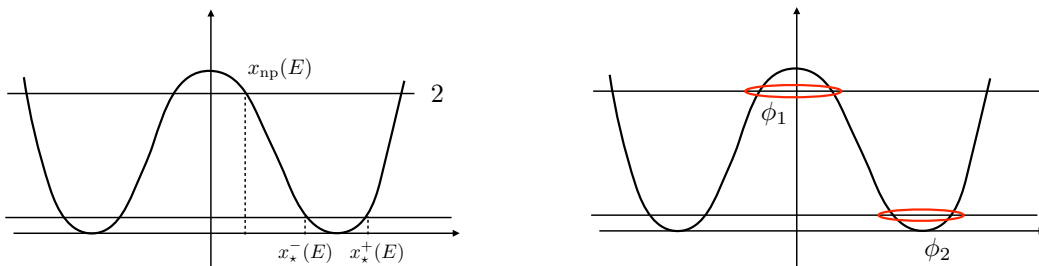


**Figure 14:** The double-well potential in the weak coupling phase. In the figure on the left we indicate the points  $x_*^\pm(E)$  and  $x_{\text{np}}(E)$ . On the figure on the right, we show the cycles that lead to the periods  $\phi_{1,2}$  in the EQC.

When  $E = 0$ , they become the critical point  $x_*$ . They are shown in Fig. 14. The classical limits  $\phi_i^{(0)}(E)$  of the quantum periods  $\phi_i$  are given by

$$\begin{aligned}\phi_1^{(0)} &= 2 \int_{x_{\text{np}}^-(E)}^{x_{\text{np}}^+(E)} \cosh^{-1}(u_4(z) - 1 - E) dz, \\ \phi_2^{(0)} &= 2 \int_{x_*^-(E)}^{x_*^+(E)} \cosh^{-1}(1 - u_4(z) + E) dz.\end{aligned}\tag{4.46}$$

Therefore,  $\phi_2^{(0)}$  is the perturbative WKB period around the critical point, while  $\phi_1^{(0)}$  is the period which appears in the weak coupling phase (the periods also depend on  $\hbar$ , but we have not indicated this dependence explicitly). The quantity  $\mathcal{V}$  is non-perturbative, and involves tunneling periods. By using the instanton expressions in [10] it can be seen that, in this phase,  $a_{1,2} > 0$ , and in addition

$$\pi a_2 = \Pi_4(E) + \mathcal{O}(\hbar^2),\tag{4.47}$$

where

$$\Pi_4(E) = 2 \int_{x_{\text{np}}^-(E)}^{x_*^-(E)} \cos^{-1}(1 - u_4(z) + E) dz + 2\pi x_{\text{np}}(E)\tag{4.48}$$

is the tunneling cycle from  $-x_*^-(E)$  to  $x_*^-(E)$ . Therefore, at leading order in both  $\hbar$  and exponentially small, non-perturbative terms, we have

$$\mathcal{V} \approx e^{-\Pi_4(E)/\hbar}.\tag{4.49}$$

We can now analyze the quantization condition (4.43) in some detail. The first observation is that, if we neglect non-perturbative corrections, we have

$$\cos\left(\frac{\phi_2}{2\hbar}\right) = 0 \Rightarrow \phi_2 = 2\pi\hbar\nu,\tag{4.50}$$

where  $\nu$  was introduced in (3.90). This is the standard all-orders Bohr–Sommerfeld quantization condition for this problem. For  $E, \hbar \rightarrow 0$ , one can see from an explicit computation of the classical period that (4.50) becomes (3.91). A second observation is that the EQC has a special solution of the form

$$\phi_1 = 2\pi\hbar\left(s + \frac{1}{2}\right), \quad \phi_2 = 2\pi\hbar\left(n + \frac{1}{2}\right)\tag{4.51}$$

where  $s$  is a non-negative integer, and  $\phi_2$  is as in (4.50). Since we have two conditions, this fixes the values of both  $E$  and  $\hbar$ . The solution is a discrete set of values for these two quantities, which are precisely the Toda lattice points mentioned in section 2. Indeed, the conditions (4.51) are a particular case of the EQCs for the periodic Toda lattice obtained in [25] for  $u(x)$  even, so these values agree with the spectrum of the corresponding conserved charges for this integrable system, in the case  $N = 4$  (the general solution for the  $N = 4$  periodic Toda lattice appears in the quantum-mechanical model with an arbitrary quartic potential.)

Let us now compute the energy gap as predicted from (4.43). To do this, we use the idea of [33]: we perturb the Bohr–Sommerfeld quantization condition (4.50) as

$$\nu = n + \frac{1}{2} + \Delta\nu, \quad (4.52)$$

where  $\Delta\nu$  is non-perturbative. One immediately finds,

$$\Delta\nu \approx -\frac{\epsilon}{\pi} \mathcal{V} \cos\left(\frac{\phi_1}{2\hbar}\right) + \mathcal{O}(\mathcal{V}^2), \quad (4.53)$$

and from here we obtain the energy gap at leading non-perturbative order:

$$\Delta E(\nu) = -\frac{2}{\pi} \frac{dE}{d\nu} e^{-\pi a_2/\hbar} \cos\left(\frac{\phi_1}{2\hbar}\right). \quad (4.54)$$

To make contact with the formula (4.10) we have to take the limit  $E, \hbar \rightarrow 0$  of this expression. In the case of  $\phi_{1,2}$ , we find immediately, after using (3.91),

$$\frac{\phi_1}{2\hbar} = \frac{\mathcal{S}_{\mathcal{I}}}{\hbar} - 2\nu \mathcal{A}_{\mathcal{I}} + \mathcal{O}(\hbar^2). \quad (4.55)$$

The limit  $E \rightarrow 0$  of (4.48) has a logarithmic singularity which has to be extracted as we have done before in e.g. (4.56). In fact, we find the same expression but involving just the real part of the action and  $\mathcal{A}$ :

$$\Pi_4(E) = \mathcal{S}_{\mathbb{R}} + \frac{E}{\omega} (\log(2E) - E) - \frac{2E}{\omega} (\mathcal{A}_{\mathcal{R}} + \log(2\omega(x_{\star} - x_0))) + \dots, \quad (4.56)$$

By using all the results, it is easy to see that the small  $\hbar$  limit of (4.54) reproduces exactly (4.10).

As noted already in [10], the energy gap vanishes and tunneling is suppressed exactly at the points (4.51). The formula (4.10) gives a small  $\hbar$  approximation to the gap, where in addition only the leading non-perturbative effect has been taken into account. The points where tunneling is suppressed can be found, at small  $\hbar$ , by determining the values of  $h$  at which the cos term vanishes, for each energy level  $n$ . It is an easy exercise to calculate this from the explicit expressions of  $\mathcal{S}_{\mathcal{I}}$ ,  $\mathcal{A}_{\mathcal{I}}$ . In particular, one has to evaluate  $\mathcal{A}_{\mathcal{I}}$  at the critical point  $h = h_c$ . In this limit, the integral defining  $\mathcal{A}_{\mathcal{I}}$  has contributions from the harmonic oscillator at  $x = x_{\star}$ , with frequency  $\omega_c = \omega(h_c)$ , and from the inverted harmonic oscillator at the local maximum at  $x = 0$ , with frequency  $\omega'_c = 2$ . One finds

$$\mathcal{A}_{\mathcal{I}}(h_c) = -\pi \frac{\omega'_c}{\omega} = -\frac{\sqrt{2}}{2} \pi, \quad (4.57)$$

and this leads to the expression

$$h_{\text{TS}} = 4 + 2 \left( s + \frac{\sqrt{2}}{2} \left( n + \frac{1}{2} \right) + \frac{1}{2} \right) \hbar + \mathcal{O}(\hbar^2), \quad (4.58)$$

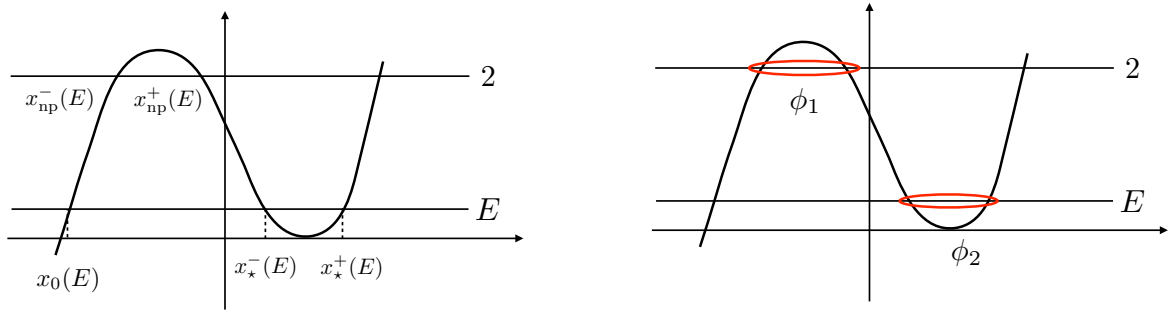


**Figure 15:** The cubic potential in the weak coupling phase. In the figure on the left we indicate the points  $x_*^\pm(E)$  and  $x_{\text{np}}^\pm(E)$ . On the figure on the right, we show the cycles that lead to the periods  $\phi_{1,2}$  appearing in the EQC.

where  $s$  corresponds to the quantum number appearing in the quantization condition of the Toda lattice (4.51). The subscript TS refers to tunneling suppression.

Let us now consider the cubic potential. In this phase, the potential looks as depicted in the figure on the left in Fig. 15. The EQC conditions read in this case

$$1 + \frac{1 - e^{-2\pi a_1/\hbar}}{1 - e^{-2\pi a_2/\hbar}} e^{i\phi_2/\hbar} - \frac{e^{-2\pi a_2/\hbar} - e^{-2\pi a_1/\hbar}}{1 - e^{-2\pi a_2/\hbar}} e^{i\phi_1/\hbar} = 0. \quad (4.59)$$

We have rearranged the periods  $a_i$  w.r.t. what is written down in [10]: the period  $a_1$  there is  $-a_1$  here, and the period  $-a_1 - a_2$  there is  $a_2$  here. With the new notation, we have in this phase  $a_1 > a_2 > 0$ . The  $B$ -periods  $\phi_1, \phi_2$  correspond to the cycles depicted in the figure on the right in Fig. 15. Their classical limits are given by the same equations as in (4.46), but with  $u_3(z)$  instead of  $u_4(z)$ . In addition, we have

$$2\pi a_2 = \Pi_3(E) + \mathcal{O}(\hbar) \quad (4.60)$$

where

$$\Pi_3(E) = 2 \left( \int_{x_0(E)}^{x_{\text{np}}^-(E)} + \int_{x_{\text{np}}^+(E)}^{x_*^-(E)} \right) \cos^{-1}(1 - u_3(z) + E) dz + 2\pi (x_{\text{np}}^+(E) - x_{\text{np}}^-(E)). \quad (4.61)$$

Let us now analyze the EQC (4.59). When all non-perturbative corrections involving  $a$  periods are neglected, we find again the all-orders Bohr–Sommerfeld quantization condition (4.50), and it is easy to see that the analogue of (4.51) solves the EQC exactly. These two equations give again the spectrum of the quantum periodic Toda lattice with  $N = 3$ . Let us now compute the imaginary part of the energy from (4.59) by considering only the leading non-perturbative correction. Since  $a_1 > a_2$ , this correction is due to  $e^{-2\pi a_2/\hbar}$ . Like before, and as in [38], we consider a perturbed Bohr–Sommerfeld solution (4.52) and we find

$$\text{Im } \Delta\nu \approx \frac{1}{2\pi} \left( 1 + \cos\left(\frac{\phi_1}{\hbar}\right) \right) e^{-2\pi a_2/\hbar}, \quad (4.62)$$

which leads in turn to

$$\text{Im } E(\nu) \approx -\frac{1}{2\pi} \frac{\partial E}{\partial \nu} \left( 1 + \cos\left(\frac{\phi_1}{\hbar}\right) \right) e^{-2\pi a_2/\hbar}. \quad (4.63)$$

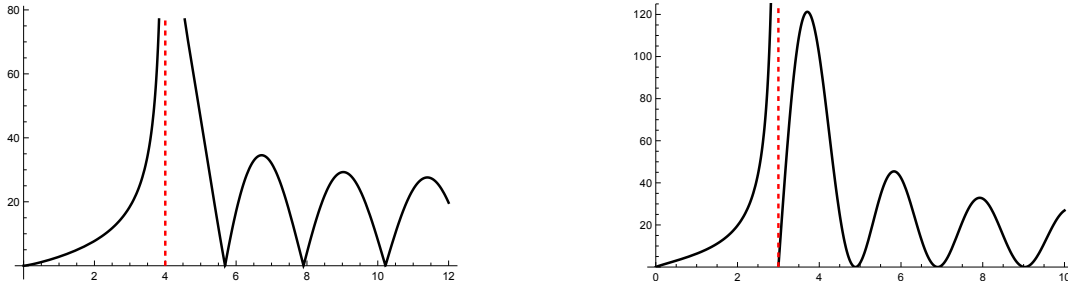


**Figure 16:** The behavior of the one-loop prefactor for the energy gap of the double well (left) and for the imaginary part of the cubic well (right), as a function of  $h$ , and we have set  $\hbar = 1$  for convenience. The red vertical lines are at  $h = h_c$ , where the functions are singular. When  $h > h_c$  they have an oscillatory behavior and tunneling is suppressed at special points.

Here we have taken into account that the EQCs of [10] give the imaginary parts of the energies of the resonances with a + sign, which is the opposite to our convention. Since in the cubic case we have

$$\frac{\phi_1}{\hbar} = \frac{\mathcal{S}_{\mathcal{I}}}{\hbar} - 2\nu\mathcal{A}_{\mathcal{I}} + \mathcal{O}(\hbar^2), \quad (4.64)$$

one finds that (4.63), in the  $\hbar \rightarrow 0$  limit, reproduces (4.34), in precise agreement with the resurgent analysis. Like in the double-well potential, we can use this formula to find the small  $\hbar$  expression for the values of  $h$  at which tunneling is suppressed. The evaluation of  $\mathcal{A}_{\mathcal{I}}$  at  $h = h_c$  is given by the same formula (4.57), but now  $\omega'_c = \omega_c = \sqrt{3}$ . We find in the end,

$$h_{\text{TS}} = 3 + \sqrt{3}(s + n + 1)\hbar + \mathcal{O}(\hbar^2). \quad (4.65)$$

## 5 The critical theories

The small  $\hbar$  asymptotics of the energy gap and the imaginary part of the energies, as a function of  $h$ , is discontinuous as we approach the critical value of the parameter  $h = h_c$ , independently of the value of  $\hbar$ . In the case of the double-well potential, the gap diverges as we approach  $h = h_c$  from both the strong and the weak coupling region, since the function  $\mathcal{A}$  in the one-loop prefactor diverges at the critical point. In the cubic well, the imaginary part of the energy diverges as we approach  $h = h_c$  from the strong coupling region, and it vanishes in the weak coupling region due to the oscillatory factor, see Fig. 16 for a graphical depiction of this behavior. Of course, in the quantum-mechanical spectral problem, the gap and the imaginary part of the energy are finite when  $h = h_c$  and for any  $\hbar > 0$ , so the discontinuity indicates rather a change of asymptotic behavior in the critical regime.

To find the critical behavior of the instanton amplitudes, we look at the WKB periods in the strong coupling phase, when  $h < h_c$ , and see what happens as we approach the critical point. Our derivation of the  $\hbar \rightarrow 0$  asymptotics in section 3.3 relied crucially on the expansion (4.56) of the tunneling period near  $E = 0$ . However, when  $h = h_c$ , this expansion is no longer valid. The reason is that there is a contribution to the logarithm coming from the inverted harmonic oscillator around the local maximum where  $u(x) = 2$ . Let us first consider the cubic potential. At the critical point  $h_c = 3$ , the correct small  $E$  expansion of the tunneling WKB period is

$$\Pi(E) = \frac{3}{\omega_c} (E \log(2E) - E) - 2\mathcal{D}_3 + \mathcal{O}(E), \quad (5.1)$$



**Figure 17:** The function  $\text{Im } \mathcal{E}(\nu, \hbar)$  evaluated on  $\hbar = 1/n$ ,  $n = 1, 2, 3, \dots$ , for  $\nu = 1/2$  (left) and  $\nu = 3/2$  (right). The red dots are numerical results, the black dots are results after applying the Richardson transform to speed up the convergence, and the blue line is the asymptotic value predicted by WKB calculation.

where  $\omega_c = \sqrt{3}$  is the value of frequency at the critical point. The factor of  $3/\omega_c$  can be understood as the contribution from one inverted oscillator at  $x = -1$ , with frequency  $\omega'_c = \omega_c$ , and half the contribution of the oscillator around  $x = x_*$  with the same frequency. The constant  $\mathcal{D}_3$  can be computed by subtracting the divergent integrals carefully as in (3.73). One finds

$$\mathcal{D}_3 = \frac{3}{2} \sqrt{3} \log(3). \quad (5.2)$$

This period then contributes to the non-perturbative amplitude as

$$e^{-\Pi(E)/\hbar} = \left( \frac{1}{2\hbar\omega_c} \right)^{3\nu} \exp \{ -3(\nu \log \nu - \nu) + 2\mathcal{D}_3\omega_c\nu + \dots \}. \quad (5.3)$$

As we mentioned in section 3.3, a crucial ingredient to obtain the correct asymptotics for a fixed energy level involves incorporating the singular part of the all-orders WKB expansion and promoting the logarithmic terms in  $\nu$  to (3.93). However, in this case, the appearance of an additional harmonic oscillator at the maximum changes this. The correct incorporation of the all-order corrections involves now

$$e^{-3(\nu \log \nu - \nu)} \rightarrow \left[ \frac{\sqrt{2\pi}}{\Gamma(\nu + \frac{1}{2})} \right]^3. \quad (5.4)$$

We have verified that this is the right correction at NLO in the WKB expansion, by using (3.97). We then obtain,

$$\text{Im } E(\nu) \approx -\frac{1}{4} \frac{\sqrt{2\pi}}{\Gamma^3(\nu + \frac{1}{2})} \left( \frac{1}{2\hbar\omega_c} \right)^{3\nu-1} e^{-\mathcal{S}_c/\hbar + 2\mathcal{D}_3\omega_c\nu}, \quad (5.5)$$

where  $\mathcal{S}_c$  is the value of the action at the critical point. In particular, when  $\nu = 1/2$  we obtain

$$\text{Im } E_0 \approx -\frac{1}{4} \left( \frac{\pi}{\hbar\omega_c} \right)^{1/2} e^{-\mathcal{S}_c/\hbar + \mathcal{D}_3\omega_c}. \quad (5.6)$$

Note that the one-loop correction scales now with  $\hbar$  as  $\hbar^{-1/2}$ , instead of  $\hbar^{1/2}$ , and the one-loop prefactor diverges as  $\hbar \rightarrow 0$ .

We can test (5.5) numerically by calculating the function

$$\text{Im } \mathcal{E}(\nu, \hbar) := -\text{Im } E(\nu, \hbar) \hbar^{3\nu-1} e^{\mathcal{S}_c/\hbar} \quad (5.7)$$

on the sequence of  $\hbar = 1/n$ ,  $n = 1, 2, 3, \dots$ , and it should have the asymptotic behavior

$$\text{Im } \mathcal{E}(\nu, 1/n) \approx \frac{1}{4} \frac{\sqrt{2\pi}}{\Gamma^3\left(\nu + \frac{1}{2}\right)} \left(\frac{1}{2\omega_c}\right)^{3\nu-1} e^{2\mathcal{D}_3\omega_c\nu} + \mathcal{O}(1/n), \quad (5.8)$$

which is indeed the case, as shown in Fig. 17.

The analysis of the double-well potential is similar. The inverted oscillator has now a frequency  $\omega'_c = 2$ , while  $\omega_c = 2\sqrt{2}$ . The tunneling period has the expansion

$$\Pi(E) = \left(\frac{1}{\omega_c} + \frac{1}{\omega'_c}\right) (E \log(2E) - E) - 2\mathcal{D}_4 + \dots \quad (5.9)$$

where

$$\mathcal{D}_4 = \frac{1}{8} \left( 8 \left( 2 + \sqrt{2} \right) \log(2) + \log \left( 17 - 12\sqrt{2} \right) - 2\sqrt{2} \log \left( 3 + 2\sqrt{2} \right) \right). \quad (5.10)$$

The contribution of the tunneling period is then

$$e^{-\Pi(E)/\hbar} \approx \left(\frac{1}{2\hbar\omega_c}\right)^{\nu\left(1+\frac{\omega_c}{\omega'_c}\right)} e^{-\left(1+\frac{\omega_c}{\omega'_c}\right)(\nu \log \nu - \nu) + 2\mathcal{D}_4\omega_c\nu}. \quad (5.11)$$

We have to find now the correct form of the all-order corrections. One indication is that the two harmonic oscillators at  $x = 0$  and  $x = \sqrt{2}$  contribute equally but with different frequencies, and the right prescription is

$$\exp \left\{ - \left( 1 + \frac{\omega_c}{\omega'_c} \right) (\nu \log \nu - \nu) \right\} \rightarrow \frac{\sqrt{2\pi}}{\Gamma\left(\nu + \frac{1}{2}\right)} \frac{\sqrt{2\pi}}{\Gamma\left(\frac{\omega_c}{\omega'_c}\nu + \frac{1}{2}\right)} \exp \left[ \frac{\omega_c}{\omega'_c} \nu \log \left( \frac{\omega_c}{\omega'_c} \right) \right], \quad (5.12)$$

which can be also verified by looking at the NLO correction. We then find for the energy splitting

$$\Delta E(\nu) \approx \left(\frac{1}{2\hbar\omega_c}\right)^{\nu\left(1+\frac{\omega_c}{\omega'_c}\right)-1} \frac{e^{-\mathcal{S}_c/\hbar}}{\Gamma\left(\nu + \frac{1}{2}\right) \Gamma\left(\frac{\omega_c}{\omega'_c}\nu + \frac{1}{2}\right)} \exp \left[ \frac{\omega_c}{\omega'_c} \nu \log \left( \frac{\omega_c}{\omega'_c} \right) + 2\mathcal{D}_4\omega_c\nu \right]. \quad (5.13)$$

For the ground state we have,

$$\Delta E_0 \approx \left(\frac{1}{2\hbar\omega_c}\right)^{\frac{\sqrt{2}-1}{2}} \frac{e^{-\mathcal{S}_c/\hbar}}{\Gamma\left(\frac{\sqrt{2}}{2} + \frac{1}{2}\right)} \exp \left[ \frac{\sqrt{2}}{4} \log(2) + \mathcal{D}_4\omega_c \right]. \quad (5.14)$$

The prefactor in the energy gap scales now with  $\hbar$  as

$$\hbar^{-\frac{\sqrt{2}-1}{2}}. \quad (5.15)$$

In general, both non-perturbative effects display an ‘‘anomalous’’ scaling as a function of  $\hbar$ , for all the levels.

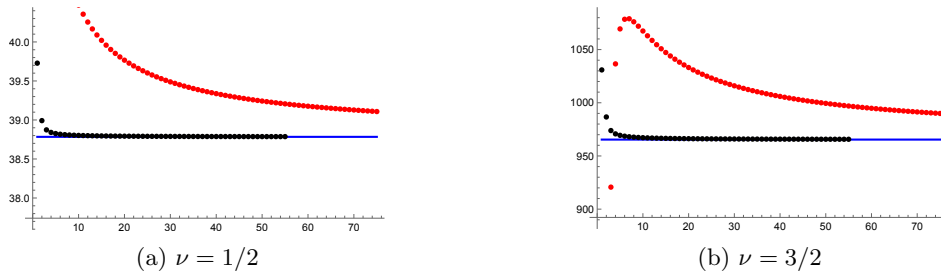


**Figure 18:** The function  $\Delta^{\mathcal{E}}(\nu, \hbar)$  evaluated on  $\hbar = 1/n$ ,  $n = 1, 2, 3, \dots$ , for  $\nu = 1/2$  (left) and  $\nu = 3/2$  (right). The red dots are numerical results, the black dots are results after applying the Richardson transform to speed up the convergence, and the blue line is the asymptotic value predicted by WKB calculation.

Similarly, we can test (5.13) numerically by calculating the function

$$\Delta^{\mathcal{E}}(\nu, \hbar) := \Delta E(\nu, \hbar) \hbar^{\left(1 + \frac{\omega_c}{\omega'_c}\right)\nu - 1} e^{S_c/\hbar} \quad (5.16)$$

on the sequence of  $\hbar = 1/n$ ,  $n = 1, 2, 3, \dots$ , and it should have the asymptotic behavior

$$\Delta^{\mathcal{E}}(\nu, 1/n) \approx \frac{(2\omega_c)^{1-\nu} \left(1 + \frac{\omega_c}{\omega'_c}\right)}{\Gamma\left(\nu + \frac{1}{2}\right) \Gamma\left(\frac{\omega_c}{\omega'_c}\nu + \frac{1}{2}\right)} \exp\left[\frac{\omega_c}{\omega'_c}\nu \log\left(\frac{\omega_c}{\omega'_c}\right) + 2\mathcal{D}_4\omega_c\nu\right] + \mathcal{O}(1/n), \quad (5.17)$$

which is indeed the case, as shown in Figs. 18.

In this derivation we have assumed that the behavior at the critical point is obtained by extrapolation from the strong coupling phase, and not from the weak coupling phase, which would give a different result. However, the detailed numerical tests show that the formulae above describe very precisely the small  $\hbar$  asymptotics of both the imaginary part of the energy in the cubic well and the energy gap in the double well. This confirms our assumption, but we lack a precise justification for this. Note that, from the point of view of the underlying  $\mathcal{N} = 2$  super Yang–Mills theory, the critical theories occur precisely at the monopole point, at the boundary between the two phases, and at point where wall-crossing takes place. The fact that the strong coupling spectrum is the one relevant to understand the quantum periods exactly at this point is reminiscent of a related observation in [50].

## 6 Conclusions

In this paper we have analyzed the behavior of the deformed quantum-mechanical models introduced in [10] from the point of view of instanton physics. Perhaps the most interesting aspect of these models is the suppression of quantum tunneling at special points in the moduli space, the so-called Toda lattice points. The instanton analysis that we have performed uncovers the physics behind tunneling suppression and unveils a rich phase structure: there is a strong coupling phase with a conventional quantum-mechanical behavior, and a weak coupling phase where the instantons become complex and lead to tunneling suppression. The two phases are separated by a critical point where the non-perturbative effects have an “anomalous” scaling. In addition, the phase structure can be regarded as a physical consequence of wall-crossing in the BPS spectrum of the underlying  $\mathcal{N} = 2$  theories.

From the purely quantum-mechanical point of view, the mechanism for tunneling suppression in our example involves complex instantons and occurs at special points in parameter space, as in [8, 9]. In contrast to these scenarios, it applies to a simpler, one-dimensional system, and the mechanism for complexification of the instantons is different and more intrinsic, since in [8, 9] tunneling suppression requires an external magnetic field. We should also point out that, in conventional quantum mechanics, changes in the parameters of the potential lead to wall-crossing and to different resurgent structures and quantization conditions, as unveiled in the pioneering works of [36, 42, 51]. However, the change in resurgent structures in that case is triggered typically by a drastic change in the classical potential, and by a rearrangement of classically allowed and forbidden zones. In the deformed quantum mechanical models that we studied in this paper, the nature of the classically forbidden region for motion in real time remains the same for all values of the control parameter  $h$ , but the motion in Euclidean time does change and alters the instanton structure.

Although the wall-crossing phenomenon is clear from a resurgent analysis of the perturbative series, it would be interesting to understand it more directly, from the point of view of the  $SU(N)$  Yang–Mills theories, and in particular in the  $SU(3)$  case, where it is richer. The connection between the wall-crossing in the spectrum and the wall-crossing in the resurgent structure studied here is however not completely direct. First, one has to connect the BPS spectrum to the resurgent structure of the WKB periods, similarly to what was done in [47], and then consider the perturbative series, which themselves involve a limiting behavior of the WKB periods akin to what was studied in [50]. The analysis of the  $SU(3)$  spectrum in e.g. [52, 53] could be a good starting point.

Another relationship that deserves further scrutiny is the connection to the EQCs found in [10]. We have found that these conditions describe correctly the small  $\hbar$  asymptotics of the non-perturbative effects for the low-lying eigenstates, but only in the weak coupling phase. The strong coupling phase is governed by a different structure. The reason is that the EQCs are expressed in terms of instanton partition sums, which are not expected to converge in the weak-coupling region  $h < h_c$ ,  $E = \mathcal{O}(\hbar)$  and  $\hbar \rightarrow 0$ . An important problem is whether the existence of such a phase structure extends to other examples. The TS/ST correspondence [13–15] provides EQCs for all the spectral problems associated to toric Calabi–Yau (CY) manifolds, and the deformed quantum-mechanical model of this paper is just one example among others. The EQCs obtained in the the TS/ST correspondence are expressed in terms of topological string partition functions at large radius, which also have a limited region of convergence. In many cases, in particular in CYs with a single modulus, this region arguably covers all possible values of the spectrum for real positive  $\hbar$ , and no phase structure seems to occur. It would be interesting to re-examine these EQCs, specially in the multi-modulus case studied in [14], to see whether similar phase structures can occur, due to a breakdown in the convergence of the partition functions involved in the EQCs. At the same time, we should emphasize that the EQCs of [10] give very explicit and detailed predictions on the non-perturbative effects appearing in the weakly-coupled phase. In this paper we have only probed the dominant ones, but the conjectural exact formulae (4.43) and (4.59) contain in principle all of them, and therefore information about the full resurgent structure (in comparing both, one has to take into account though that the quantum periods appearing in the instanton sums and the ones in the exact WKB method might be different, as shown in [47]).

Although we have focused on the most emblematic cases, the double well and the cubic potential, it would be interesting to find a general pattern for potentials of higher degree, where these phenomena also occur. Recently, based on the open string version of the TS/ST correspondence

[54–57], exact expressions for the eigenfunctions of the deformed quantum-mechanical models of [10] have been found in [58]. It would be very interesting to examine the phase structure found in this paper from the point of view of these wavefunctions.

Another interesting problem is to develop more rigorous methods to study the type of difference equations that appear in deformed quantum mechanics, and perhaps prove rigorously some of the results in [10] and in this paper. For example, the asymptotic behavior of the energy gap in double-well systems has been derived rigorously (see [59] for a classic paper and [9] for more recent results). The phase structure found in this paper, and in particular the “anomalous” scaling at the critical point, seem ideal laboratories to extend the spectral theory of the energy gap. In another direction, developing the exact WKB approach to these equations along the lines of [19, 20] might lead to a derivation of both the EQCs of [10] and to a derivation of the phase structure uncovered here. Recent results on wavefunctions of the Baxter operator of the Todal lattice [60] might be also useful in that respect.

## Acknowledgements

M.M. would like to thank Slava Rychkov for reigniting his interest in this problem. We thank Paulo Mourão for initial collaboration in this project in 2022, and Alba Grassi and Nils Wagner for useful discussions. We also thank Alba Grassi for a critical reading of the manuscript. The work of M.M. was supported in part by the ERC-SyG project “Recursive and Exact New Quantum Theory” (ReNewQuantum), which received funding from the European Research Council (ERC) under the European Union’s Horizon 2020 research and innovation program, grant agreement No. 810573. The work of J.G. is supported in part by the NSF of China through Grant No. 12375062.

## References

- [1] E. Merzbacher, *The early history of quantum tunneling*, *Physics Today* **55** (Aug., 2002) 44–49.
- [2] M. Mariño, *Advanced Topics in Quantum Mechanics*. Cambridge University Press, 12, 2021, [10.1017/9781108863384](https://doi.org/10.1017/9781108863384).
- [3] M. Mariño, *Instantons and large  $N$ . An introduction to non-perturbative methods in quantum field theory*. Cambridge University Press, 2015.
- [4] B. Garbrecht and N. Wagner, *Instantons meet resonances: Unifying two seemingly distinct approaches to quantum tunneling*, [2512.04907](https://arxiv.org/abs/2512.04907).
- [5] B. Garbrecht and N. Wagner, *Path integral analysis of Schrödinger-type eigenvalue problems in the complex plane: Establishing the relation between instantons and resonant states*, [2507.23125](https://arxiv.org/abs/2507.23125).
- [6] F. Grossmann, T. Dittrich, P. Jung and P. Hänggi, *Coherent destruction of tunneling*, *Phys. Rev. Lett.* **67** (Jul, 1991) 516–519.
- [7] D. Loss, D. P. DiVincenzo and G. Grinstein, *Suppression of tunneling by interference in half-integer-spin particles*, *Phys. Rev. Lett.* **69** (Nov, 1992) 3232–3235.
- [8] A. Garg, *Topologically quenched tunnel splitting in spin systems without Kramers’ degeneracy*, *Europhysics Letters* **22** (apr, 1993) 205.
- [9] C. L. Fefferman, J. Shapiro and M. I. Weinstein, *Quantum tunneling and its absence in deep wells and strong magnetic fields*, *Proceedings of the National Academy of Sciences* **122** (2025) [e2420062122](https://doi.org/10.1073/pnas.2420062122), [<https://www.pnas.org/doi/pdf/10.1073/pnas.2420062122>].
- [10] A. Grassi and M. Mariño, *A solvable deformation of quantum mechanics*, *SIGMA* **15** (2019) 025, [[1806.01407](https://arxiv.org/abs/1806.01407)].
- [11] E. J. Martinec and N. P. Warner, *Integrable systems and supersymmetric gauge theory*, *Nucl. Phys. B* **459** (1996) 97–112, [[hep-th/9509161](https://arxiv.org/abs/hep-th/9509161)].

- [12] N. Seiberg and E. Witten, *Electric-magnetic duality, monopole condensation, and confinement in  $N=2$  supersymmetric Yang-Mills theory*, *Nucl. Phys. B* **426** (1994) 19–52, [[hep-th/9407087](#)].
- [13] A. Grassi, Y. Hatsuda and M. Mariño, *Topological strings from quantum mechanics*, *Annales Henri Poincaré* **17** (2016) 3177–3235, [[1410.3382](#)].
- [14] S. Codesido, A. Grassi and M. Mariño, *Spectral theory and mirror curves of higher genus*, *Annales Henri Poincaré* **18** (2017) 559–622, [[1507.02096](#)].
- [15] X. Wang, G. Zhang and M.-x. Huang, *New exact quantization condition for toric Calabi–Yau geometries*, *Phys. Rev. Lett.* **115** (2015) 121601, [[1505.05360](#)].
- [16] M. R. Douglas and S. H. Shenker, *Dynamics of  $SU(N)$  supersymmetric gauge theory*, *Nucl. Phys. B* **447** (1995) 271–296, [[hep-th/9503163](#)].
- [17] R. B. Dingle and G. J. Morgan, *WKB methods for difference equations I*, *Applied Scientific Research* **18** (1968) 221–237.
- [18] A. Klemm, W. Lerche, S. Yankielowicz and S. Theisen, *Simple singularities and  $N=2$  supersymmetric Yang-Mills theory*, *Phys. Lett. B* **344** (1995) 169–175, [[hep-th/9411048](#)].
- [19] F. Del Monte and P. Longhi, *Monodromies of Second Order  $q$ -difference Equations from the WKB Approximation*, [2406.00175](#).
- [20] S. Baldino, *WKB Methods for Finite Difference Schrodinger Equations*. PhD thesis, Lisbon, IST Maths, 2023. [2410.14628](#).
- [21] L. Bramley, L. Hollands and S. Murugesan, *Les Houches lectures on non-perturbative Seiberg-Witten geometry*, [2503.21742](#).
- [22] M. Mariño, *Spectral theory and mirror symmetry*, [1506.07757](#).
- [23] A. Laptev, L. Schimmer and L. A. Takhtajan, *Weyl asymptotics for perturbed functional difference operators*, *J. Math. Phys.* **60** (2019) 103505, [10](#).
- [24] A. Laptev, L. Schimmer and L. A. Takhtajan, *Weyl type asymptotics and bounds for the eigenvalues of functional-difference operators for mirror curves*, *Geom. Funct. Anal.* **26** (2016) 288–305, [[1510.00045](#)].
- [25] N. A. Nekrasov and S. L. Shatashvili, *Quantization of Integrable Systems and Four Dimensional Gauge Theories*, [0908.4052](#).
- [26] A. Losev, N. Nekrasov and S. L. Shatashvili, *Testing Seiberg-Witten solution*, *NATO Sci. Ser. C* **520** (1999) 359–372, [[hep-th/9801061](#)].
- [27] N. A. Nekrasov, *Seiberg-Witten prepotential from instanton counting*, *Adv. Theor. Math. Phys.* **7** (2003) 831–864, [[hep-th/0206161](#)].
- [28] M. Gaudin and V. Pasquier, *The periodic Toda chain and a matrix generalization of the Bessel function’s recursion relations*, *J. Phys. A* **25** (1992) 5243.
- [29] K. Kozłowski and J. Teschner, *TBA for the Toda chain*, [1006.2906](#).
- [30] J. Zinn-Justin, *Quantum field theory and critical phenomena*, vol. 85 of *International Series of Monographs on Physics*. The Clarendon Press, Oxford University Press, New York, second ed., 1993.
- [31] L. A. Takhtajan, *Quantum mechanics for mathematicians*. American Mathematical Society, Providence, RI, 2008.
- [32] K. Iwaki, *Les Houches Lectures on Exact WKB Analysis and Painlevé Equations*, [2512.17599](#).
- [33] G. Álvarez, *Langer–Cherry derivation of the multi-instanton expansion for the symmetric double well*, *J. Math. Phys.* **45** (2004) 3095–3108.
- [34] L. D. Landau and E. M. Lifshitz, *Quantum mechanics. Non-relativistic theory*. Pergamon Press, 1958.
- [35] A. Garg, *Tunnel splittings for one dimensional potential wells revisited*, *Am. J. Phys.* **68** (2000) 430, [[cond-mat/0003115](#)].

- [36] E. Delabaere, H. Dillinger and F. Pham, *Exact semiclassical expansions for one-dimensional quantum oscillators*, *J. Math. Phys.* **38** (1997) 6126–6184.
- [37] D. Gaiotto, *Opers and TBA*, [1403.6137](#).
- [38] G. Álvarez and C. Casares, *Exponentially small corrections in the asymptotic expansion of the eigenvalues of the cubic anharmonic oscillator*, *J. Phys.* **A33** (2000) 5171.
- [39] K. Ito, M. Mariño and H. Shu, *TBA equations and resurgent Quantum Mechanics*, *JHEP* **01** (2019) 228, [[1811.04812](#)].
- [40] E. Brezin, J. C. Le Guillou and J. Zinn-Justin, *Perturbation Theory at Large Order. 2. Role of the Vacuum Instability*, *Phys. Rev. D* **15** (1977) 1558–1564.
- [41] R. Balian, G. Parisi and A. Voros, *Quartic oscillator*, in *Feynman Path Integrals*, vol. 106, pp. 337–360. Springer-Verlag, 1979.
- [42] A. Voros, *The return of the quartic oscillator. The complex WKB method*, *Annales de l'I.H.P. Physique Théorique* **39** (1983) 211–338.
- [43] H. J. Silverstone, *JWKB connection-formula problem revisited via Borel summation*, *Phys. Rev. Lett.* **55** (1985) 2523.
- [44] T. Sulejmanpasic and M. Ünşal, *Aspects of perturbation theory in quantum mechanics: The BenderWu Mathematica  $\text{\textcircled{R}}$  package*, *Comput. Phys. Commun.* **228** (2018) 273–289, [[1608.08256](#)].
- [45] Z. Duan, J. Gu, Y. Hatsuda and T. Sulejmanpasic, *Instantons in the Hofstadter butterfly: difference equation, resurgence and quantum mirror curves*, *JHEP* **01** (2019) 079, [[1806.11092](#)].
- [46] F. Ferrari and A. Bilal, *The Strong coupling spectrum of the Seiberg-Witten theory*, *Nucl. Phys. B* **469** (1996) 387–402, [[hep-th/9602082](#)].
- [47] A. Grassi, J. Gu and M. Mariño, *Non-perturbative approaches to the quantum Seiberg-Witten curve*, *JHEP* **07** (2020) 106, [[1908.07065](#)].
- [48] G. V. Dunne and M. Ünşal, *Uniform WKB, Multi-instantons, and Resurgent Trans-Series*, *Phys. Rev. D* **89** (2014) 105009, [[1401.5202](#)].
- [49] A. Matsuyama, *Periodic Toda lattice in quantum mechanics*, *Annals of Physics* **220** (1992) 300–334.
- [50] M. Mariño and M. Schwick, *Large  $N$  instantons, BPS states, and the replica limit*, [2403.14462](#).
- [51] E. Delabaere, H. Dillinger and F. Pham, *Résurgence de Voros et périodes des courbes hyperelliptiques*, *Annales de l'institut Fourier* **43** (1993) 163–199.
- [52] D. Galakhov, P. Longhi, T. Mainiero, G. W. Moore and A. Neitzke, *Wild Wall Crossing and BPS Giants*, *JHEP* **11** (2013) 046, [[1305.5454](#)].
- [53] F. Yan, *Exact WKB and the quantum Seiberg-Witten curve for 4d  $N = 2$  pure  $SU(3)$  Yang-Mills. Abelianization*, *JHEP* **03** (2022) 164, [[2012.15658](#)].
- [54] M. Mariño and S. Zakany, *Exact eigenfunctions and the open topological string*, *J. Phys. A* **50** (2017) 325401, [[1606.05297](#)].
- [55] M. Mariño and S. Zakany, *Wavefunctions, integrability, and open strings*, *JHEP* **05** (2019) 014, [[1706.07402](#)].
- [56] M. François and A. Grassi, *Painlevé Kernels and Surface Defects at Strong Coupling*, *Annales Henri Poincaré* **26** (2025) 2117–2172, [[2310.09262](#)].
- [57] M. François and A. Grassi, *On the open TS/ST correspondence*, [2503.21762](#).
- [58] M. François, A. Grassi and T. Pedroni, *Eigenfunctions of deformed Schrödinger equations*, [2511.10636](#).
- [59] B. Simon, *Semiclassical analysis of low lying eigenvalues. II. Tunneling*, *Ann. of Math. (2)* **120** (1984) 89–118.
- [60] J. Baerman, G. Ravazzini and J. Teschner, *Higher-Rank Mathieu Opers, Toda Chain, and Analytic Langlands Correspondence*, [2512.18744](#).